10-1-2008

PCI/NSF Development Of A Design Methodology For Precast Concrete Diaphragms Half Scale Connector Performance, Phase 1c

Clay Naito

Ruirui Ren

PCI/NSF
DEVELOPMENT OF A DESIGN METHODOLOGY FOR PRECAST CONCRETE DIAPHRAGMS

CONNECTOR PERFORMANCE
PHASE 1C-HALF SCALE

By

Clay Naito
Ruirui Ren

October 2008

ATLSS REPORT NO. 08-09

ATLSS is a National Center for Engineering Research on Advanced Technology for Large Structural Systems

117 ATLSS Drive

Bethlehem, PA 18015-4729

Phone: (610)758-3525
Fax: (610)758-5902

www.atlss.lehigh.edu
Email: inatl@lehigh.edu

1. ACKNOWLEDGEMENTS

This research is part of the PCI/NSF collaborative research project "Development of A Seismic Design Methodology for Floor Diaphragms" organized by Robert Fleischman at the University of Arizona, Clay Naito and Richard Sause at Lehigh University, and Jose Restrepo at the University of California San Diego. This project was financed in part by a grant from the Commonwealth of Pennsylvania, Department of Community and Economic development, through the Pennsylvania Infrastructure Technology Alliance (PITA), and through support from the Precast and Prestressed Concrete Institute (PCI), the US National Science Foundation (NSF) and the contributions of Tindall Corporation and the Shockey Precast Group. The authors would also like to thank the DSDM advisory board for development of the testing program and review of this document.

2. ABSTRACT

This report summarizes the in-plane performance of Phase 1C half scale connectors. The connectors were tested at half scale to replicate the details used in a shake table specimen examined at the University of California San Diego and the Phase 2 joint tests conducted at Lehigh University. The connectors are used to provide integrity between precast concrete double tee panel flanges. Both pre-topped and topped flanges were examined. All tests were conducted under deformation based protocols including cyclic tension, cyclic shear and cyclic shear with constant opening. The resulting capacities and associated damage are summarized in the report. This work was conducted at the ATLSS Center at Lehigh University. The following connectors were evaluated as part of this test series.

- JVI Vector Connector
- Topped Hairpin with Ductile Ladder
- Pre-topped Carbon Chord Connector

3. TABLE OF CONTENTS

4. BACKGROUND

As a means of assessing the displacement capacity and structural stiffness of connections in precast diaphragms, an experimental study was conducted. A subassembly consisting of the connector and a portion of the surrounding diaphragm was developed. The subassemblies include two connectors embedded in standard precast concrete panels. All specimens were fabricated at half-scale unless otherwise noted. This report summarizes the experimental results of a number of connectors tested under displacement control in cyclic tension, cyclic shear, and cyclic shear with constant opening.

4.1. Subassembly Details

The subassembly consist of a portion of a double tee floor diaphragm 8ft long and 4ft DT web to the free flange face. The test specimens are fabricated from two half scale panels measuring 2ft wide and 4ft long (Figure 4-1). The panels are connected to form a 4ft square subassembly. Welded wire reinforcement (WWR) is included in each panel to meet ACI [1] temperature and shrinkage reinforcement requirements. In addition to the WWR conventional reinforcement is used to maintain integrity during testing. The bars are placed at the periphery of the panel to minimize influence on the connector response. The supplemental reinforcement is illustrated in Figure 4-2.

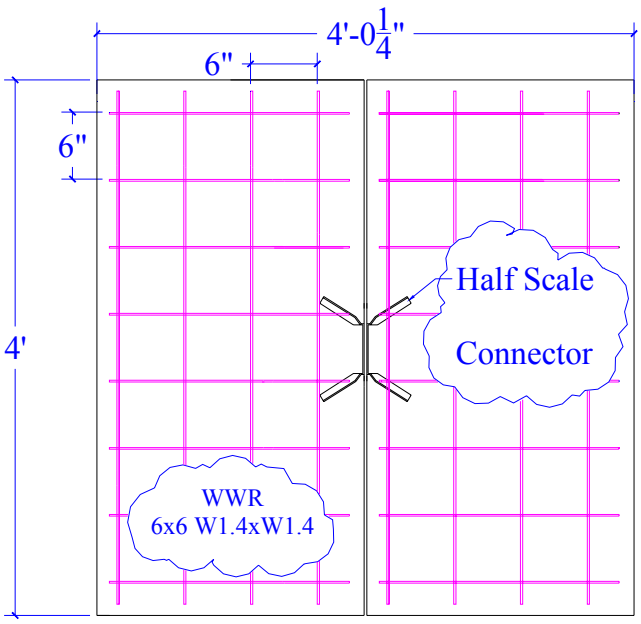

Figure 4-1: Specimen details

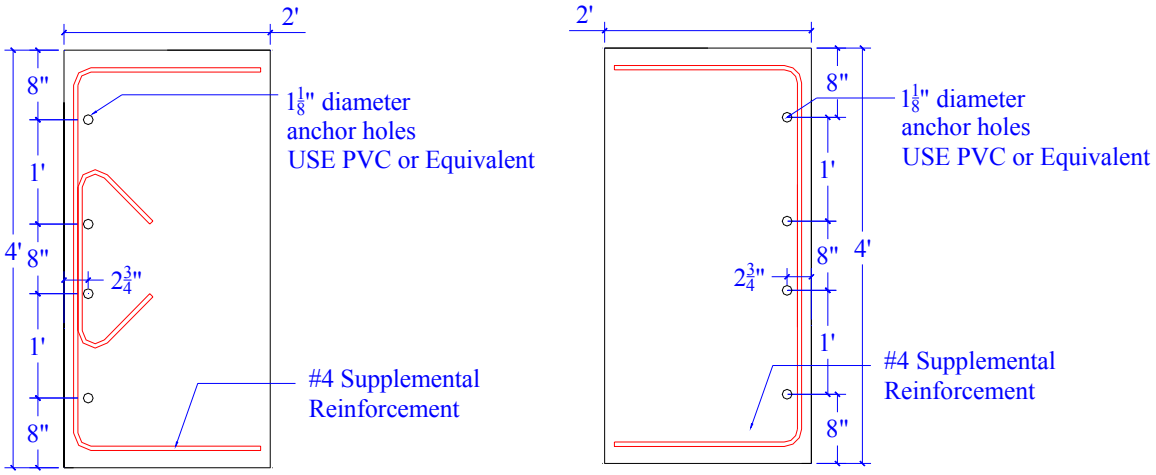

a) For JVI and Hairpin Connectors b) For Chord Connectors

Figure 4-2: Supplemental reinforcement layout and construction details

4.2. Loading Protocols

4.2.1 Deformation Based Protocols

The connectors are evaluated under in-plane shear and tension. All tests were conducted under quasi-static displacement control at a rate less than 0.05in/sec. The tests were continued until failure. Failure is defined as the point where the specimen capacity drops below 25% of the measured ultimate. The displacement protocols have been developed to represent the spectrum of demands a local diaphragm connector could experience under lateral loading [Naito 2005]. For this phase half scale tests, these protocols will be used:

1. Cyclic Tension
2. Cyclic Shear
3. Cyclic Shear with Constant Opening

4.2.1.1 Cyclic Tension

The cyclic response of the connection to opening and closing will be assessed with a cyclic tension test. The test consists of three elastic levels of 0.25Δ, 0.50Δ and 0.75Δ followed by inelastic cycles to 1.0Δ, 1.5Δ, 2.0Δ, 3.0Δ, 4.0Δ, 6.0Δ, 8.0Δ, *etc.*.. The protocol is shown in Figure 4-3. The compression cycle consisted of a closing displacement of 0.01-in. The shear actuator will be disconnected for the tests. This will result in zero shear force and allows small shear deformations.

4.2.1.2 Cyclic Shear

Cyclic shear tests provide insight on the degradation of shear properties (i.e., stiffness and ultimate strength) under loading reversals. The loading protocol is based on the PRESSS program [Priestley 1992] [2]. Three preliminary cycles to 0.01-in. will be conducted to evaluate control and acquisition accuracy. The remaining protocol consisted of groups of three symmetric shear cycles at increasing deformation levels. Each level is based on a percentage of a reference deformation computed from the preceding monotonic test. The reference deformation represents half of the effective yield deformation of the half scale connector. It is assumed as half of the intercept of a horizontal line at the max load and a secant stiffness line at 75% of the max load (Figure 4-4 inset). Three elastic levels of 0.25Δ, 0.50Δ and 0.75Δ followed by inelastic cycles to 1.0Δ, 1.5Δ, 2.0Δ, 3.0Δ, 4.0Δ, 6.0Δ, 8.0Δ, *etc.*.. will be conducted. The loading protocol is illustrated in Figure 4-4.

4.2.1.3 Cyclic Shear with Constant Opening

The cyclic shear response of the connection with constant opening will be assessed with this test protocol. The test consists of three elastic levels of 0.25Δ, 0.50Δ and 0.75Δ followed by inelastic cycles to 1.0Δ, 1.5Δ, 2.0Δ, 3.0Δ,

4.0⊿, 6.0⊿, 8.0⊿, *etc…* The panel was subjected to shear displacement with a constant tension opening of ΔT = 0.10-in. in the positive shear direction.

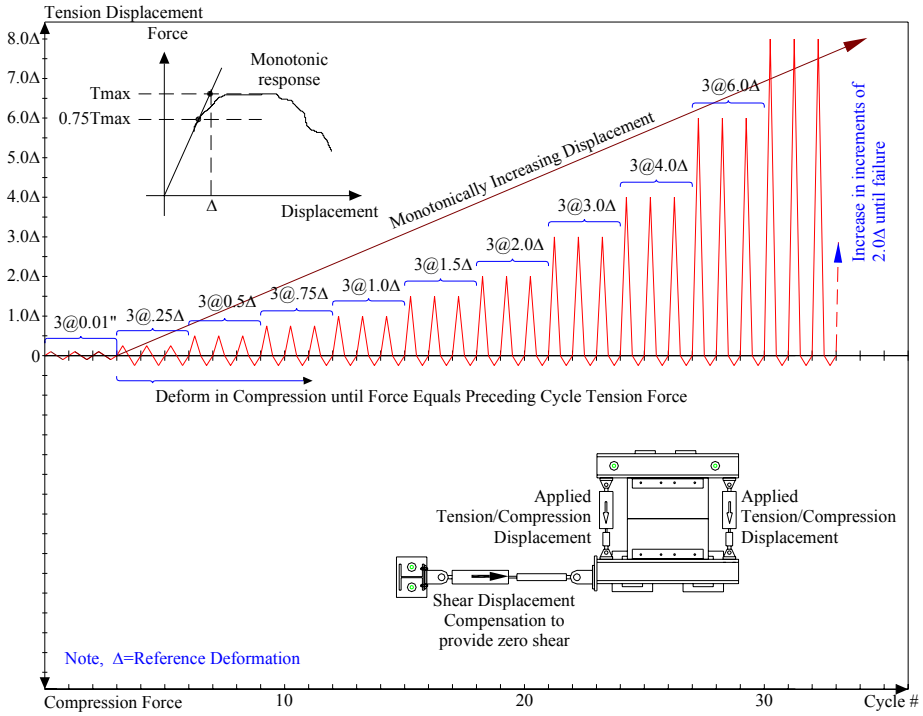

Figure 4-3: Tension loading protocol

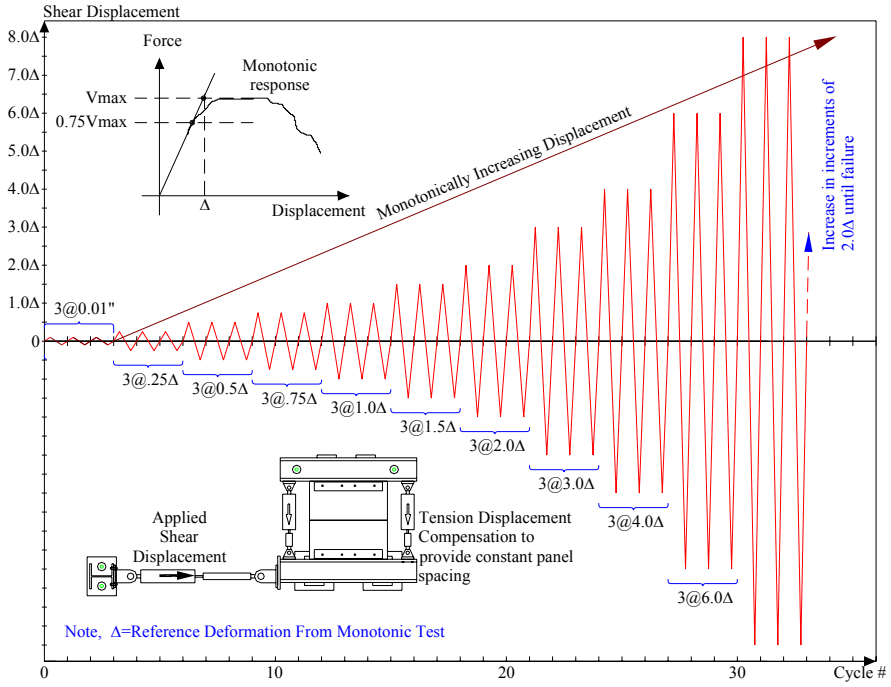

Figure 4-4: Shear loading protocol

4.3. Instrumentation Layout

Linear voltage displacement transducers (LVDT) are used to acquire information about the local joint and global displacements, as shown in Figure 4-6: seven LVDTs (C1 through C7) are used to measure the axial displacements; and one LVDT (C8) is used to measure the shear displacement. C1 ~ C3 and C4 ~ C6 are located symmetrically at each side of the connection to measure the local joint axial displacements and panel deformation. C2 and C5 are located at 12-in from the centerline of the connection on each side to measure the local joint axial displacement; the gage length for both of them is 12-in. LVDTs C1, C3, C4 and C6 are used to measure the panel deformation, all these LVDTs are located at 18-in from the edge of the each beam. C7 is located at the centerline of the connection. The layout of all the LVDTs used on the panel is as shown in during the test.

Besides the External LVDTs used on the panel, Temposonic transducers were used between each beam to control the applied deformation, they were centered pin to pin of each actuator (Figure 4-6). Through the remainder of the report the term "Temposonic Data" denotes the average displacement recorded by Temposonic transducers mounted on Actuator 2 and 3 for tension tests; for the shear tests, it denotes the data attained from Temposonic transducer of Shear actuator 1. The term "LVDT Data" in the later text and figures denotes the average opening displacement measured on LVDTs C2, C5 and C7.

It was observed that the "Temposonic Data" matched well with "LVDT Data" (see Figure 5-4). Unlike the Temposonic transducers the LVDT transducers measured the behavior at the joint. The Temposonic transducers measured not only the joint response but the deformation of the concrete panels away from the joint and any slip at the connections between the panel reaction frame. To simplify reporting the "LVDT Data" was chosen to represent the connector performance in the figures unless the LVDT was lost prematurely due to panel damage during the test.

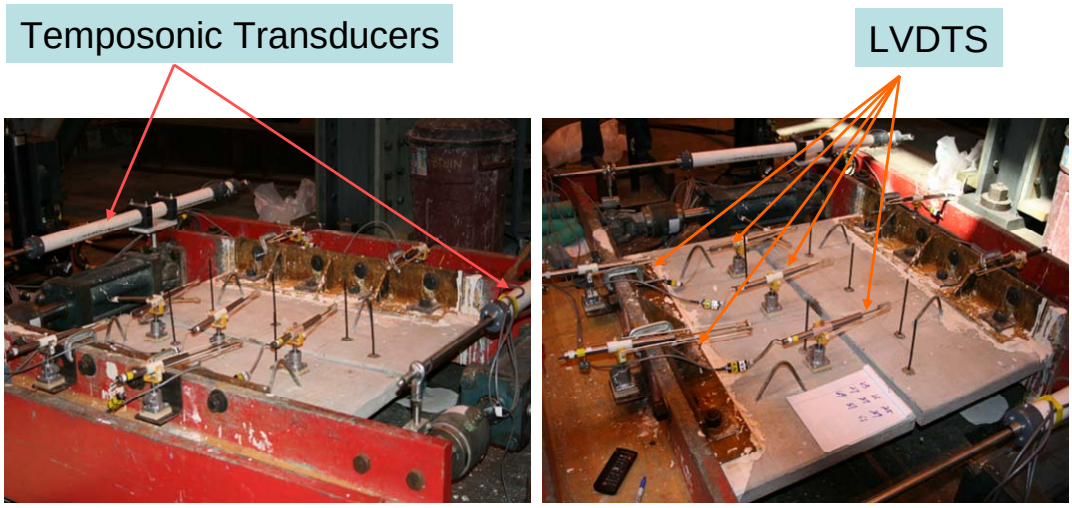

Figure 4-5: LVDT layout

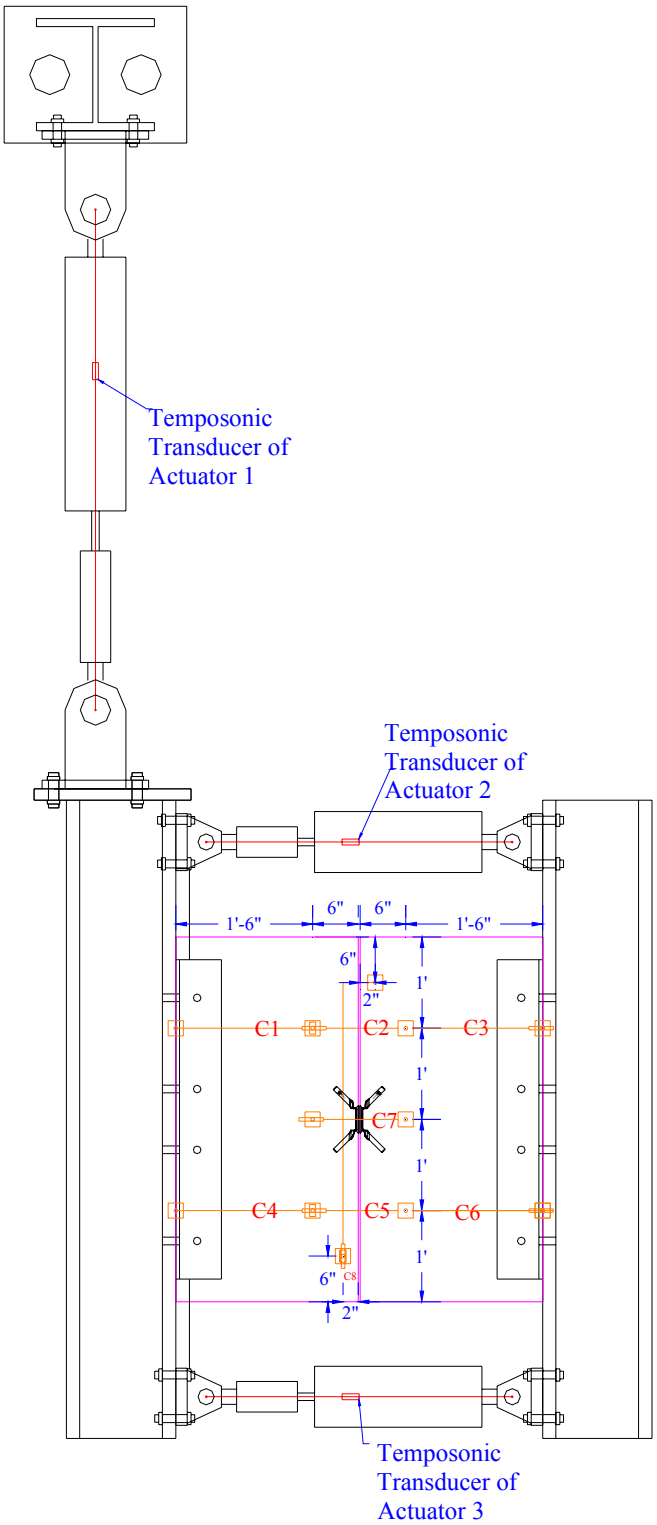

Figure 4-6: Instrumentation Detail for Half-scale Test

4.4. Backbone Approximation

For all the experimental data, a smooth "backbone" curve was drawn through each point of peak displacement during the first cycle of each increment of loading (or deformation) as indicated in ASCE/SEI41-06[3].This method provides a higher estimate of load than the previously used method outlined in FEMA356, in which the "backbone" curve is defined by drawing through the intersection of the first cycle curve for all the (i)th deformation step with the second cycle curve of (i-1)th deformation step[4].The difference between the two methods is illustrated in Figure 4-7[5].

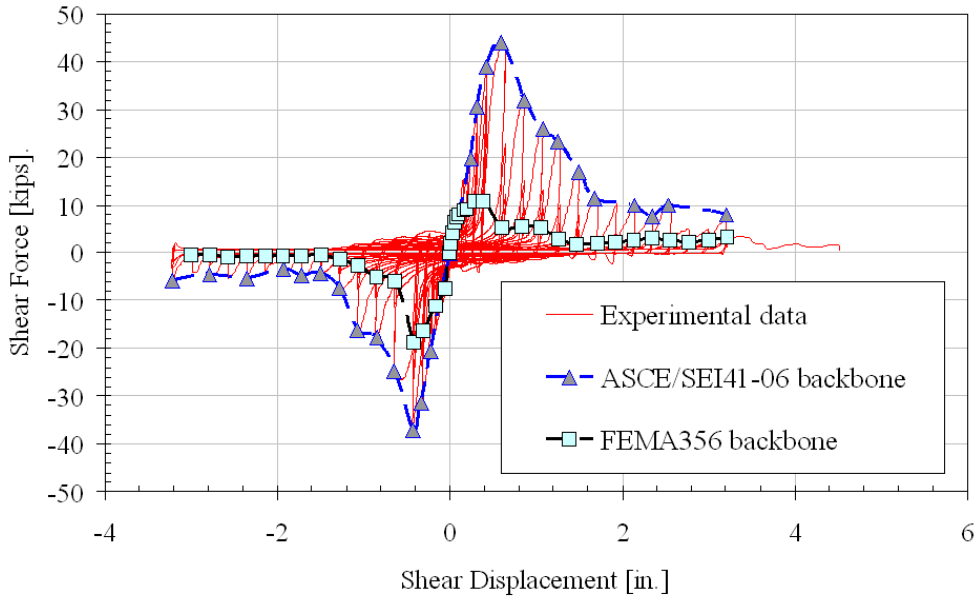

Figure 4-7: Backbone curve

5. TYPE O: HALF SCALE JVI VECTOR CONNECTOR

The specimen tested represents a JVI Vector connection used as a connector between double tee panels. A 2-in thick pre-topped flange was chosen to represent half scale of a typical 4-in pre-topped floor diaphragm system used in low seismic zones. The connectors were fabricated exactly at half scale through the assistance of JVI Corporation as indicated in Figure 5-1.

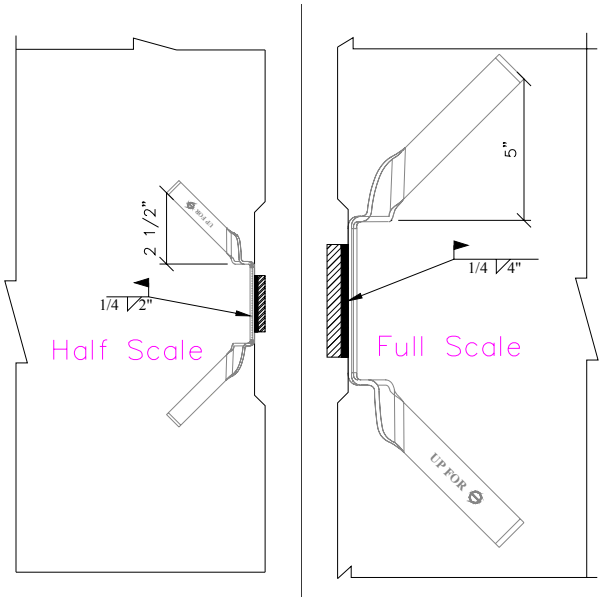

Figure 5-1 Scaling of JVI Vector Connection

The connectors were welded to a 1.75-in. x 1-in. x 3/16-in.rectangular slug, which is an exact half scale of a standard full-scale slug used in previous test series. Details of the specimen are shown in Figure 5-2.

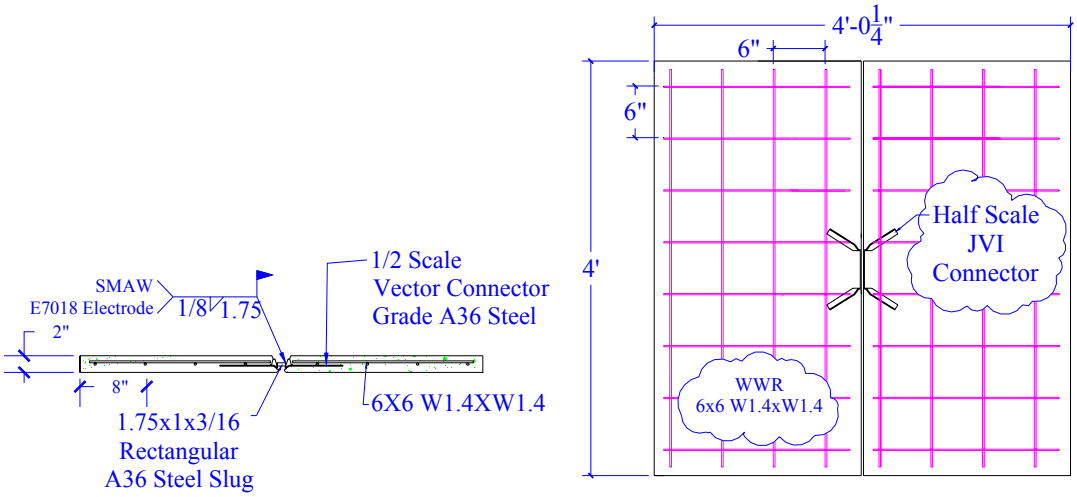

Figure 5-2: JVI Vector Connection

5.1. Material Properties JVI Connectors

The 2-in. precast panels were fabricated with a design compressive strength of 5000 psi at 28 days. The WWR used in the base panel met the requirements of ASTM A185 grade 65 steel. The connectors were furnished by JVI. Material data supplied with the connectors indicated that the JVI connector was fabricated from A-36 steel coated

with J-finish to protect the connector from corrosion, plate properties were not available. The slugs were fabricated from ASTM A-36 steel. All welds were conducted using the shielded metal arc welding (SMAW) process using E7018 electrodes in accordance with AWS standards [6]. The compressive strength of the concrete when the panel tests were conducted was measured in accordance with ASTM C39. The measured concrete strengths and mill certified steel properties are presented in Table 5-1.

Table 5-1: Material Properties Capacity

Concrete Panel Type	Compressive Strength, f'c [psi]			
2-in.	6583 ±92			
Size	Reinforcement Usage	Grade	Yield Stress [ksi]	Ultimate Strength [ksi]
PL 3/16" x 1" x 1.75"	Slug	A36	47.9	69.7
#4	Reinforcing Bars	A615 Gr. 60	67.7	105.4
6X6 W1.4XW1.4	Pre-cast Panel Mesh	A185 Gr.65	65.00*	108.5
* Data unavailable, value assumed				

5.2. Type O-1: Half Scale JVI Cyclic Tension Deformation with Fv = 0

The performance of the half scale JVI-Vector connection subjected to cyclic tension and compression is presented in this section. The panel was subjected to axial displacement with the shear displacement unrestrained, Fv=0. A reference tension deformation of 0.0525 was used for the test, this value was based on the effective yield deformation of the half scale JVI connector, which was computed as half of the intercept of a horizontal line at the max load and a secant stiffness line at 75% of the max load of the full scale JVI connector under the monotonic tension loading protocol. Panel damage initiated with cracking of the concrete panels over the connector. Throughout the test the faceplate of the connector would pull away under tension, and bear against the panel in compression. This behavior resulted in repetitive bending of the faceplate and a low cycle fatigue failure at the interface between the faceplate and the anchorage leg. The right leg fractured at an opening 0.525-in. and the left leg fractured at 0.735-in. Observed key events and the corresponding displacement level are presented in Table 5-2. The photos of the damage are presented in Figure 5-3.The global force deformation response and backbone curve are presented in Table 5-3 and Figure 5-5. All results are presented as measured. To compare with full scale response, displacements should be multiplied by 2.0 and forces by 4.0.

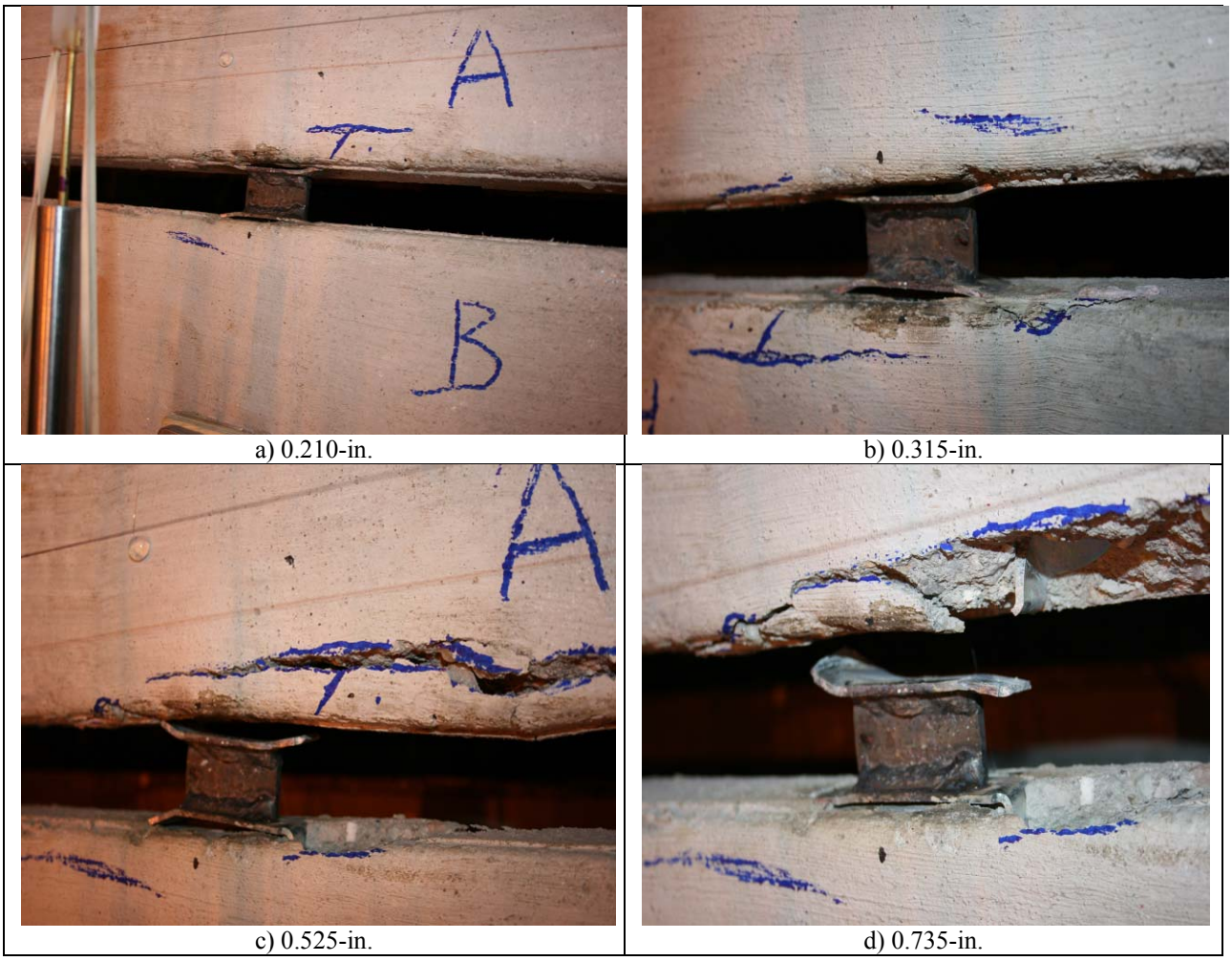

a) 0.210-in. b) 0.315-in.

c) 0.525-in. d) 0.735-in.

Figure 5-3: Damage state at various axial deformations.

Table 5-2: Experimental observation of JVI Vector Connector (Cyclic Tension)		
Event #	Tensile Δ [in.]	Event Description
1	0.026	Small Gap between Connector Plates and Panel B
2	0.039	Small Gaps between Connector Plates and Panel B and Panel A
3	0.210	Horizontal Crack over the Right Connector Leg on Panel A and Left Connector Leg on Panel B
4	0.315	Crack on Panel B Elongated and Extending Down through Panel Face
5	0.525	Right Leg of Connection on Panel A Fully Fractured
6	0.630	Concrete in Front of Right Connector Leg of Panel A Spalled
7	0.735	Left Leg of Connection on Panel A Fully Fractured

Table 5-3: Experimental Results Backbone JVI Vector Connector (Cyclic Tension)		
Event	Axial Displacement [in.]	Axial Force [kips]
-	0	0
-	0.019	1.624
- Small Gaps between Connector Plates and Panel B	0.024	1.682

Table 5-3: Experimental Results Backbone JVI Vector Connector (Cyclic Tension)		
- Small Gaps between Connector Plates and Panel B and Panel A	0.036	1.824
-	0.061	2.009
-	0.076	2.030
-	0.102	2.124
	0.159	2.257
- Horizontal Crack over the Right Connector Leg on Panel A and Left Connector Leg on Panel B	0.214	2.286
- Peak Load & Crack on Panel B Elongated and Extending Down through Panel Face	0.305	2.339
	0.415	2.249
- Right Leg of Connection on Panel A Fully Fractured	0.512	2.106
- Concrete in Front of Right Connector Leg of Panel A Spalled	0.610	1.009

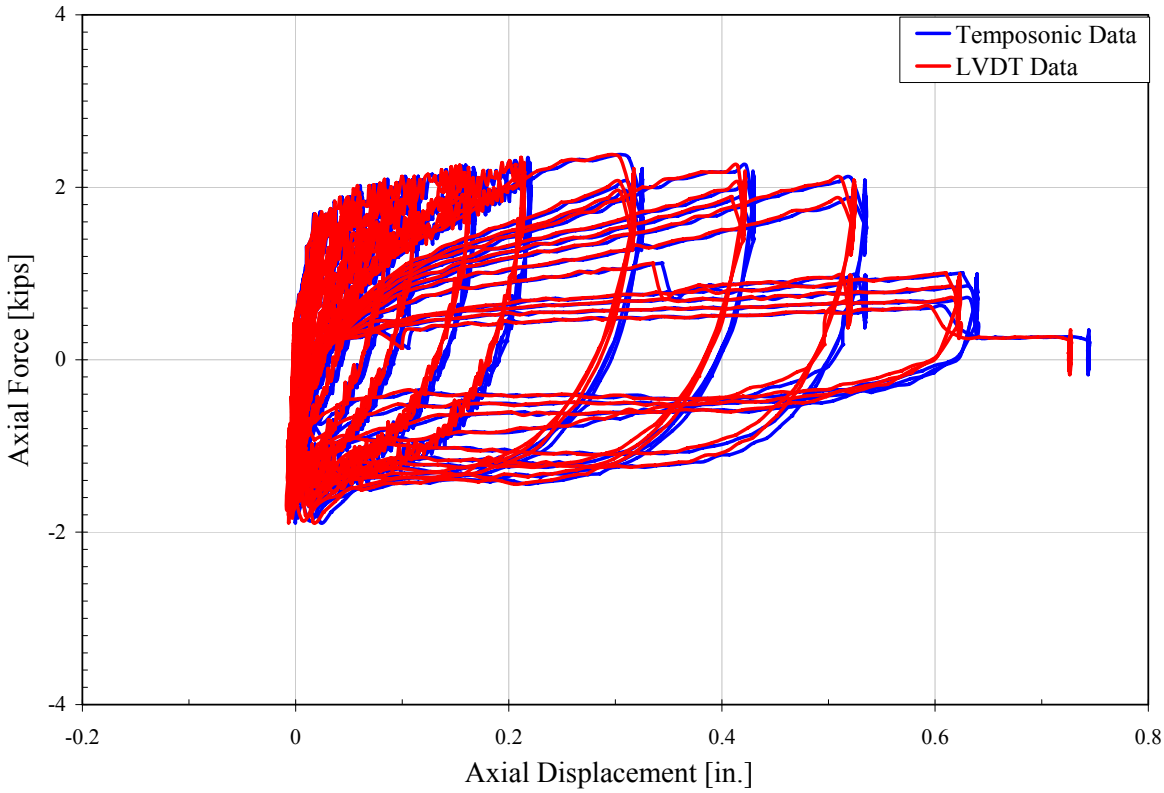

Figure 5-4: Temposonic Data and LVDT Data for JVI cyclic Tension Tests

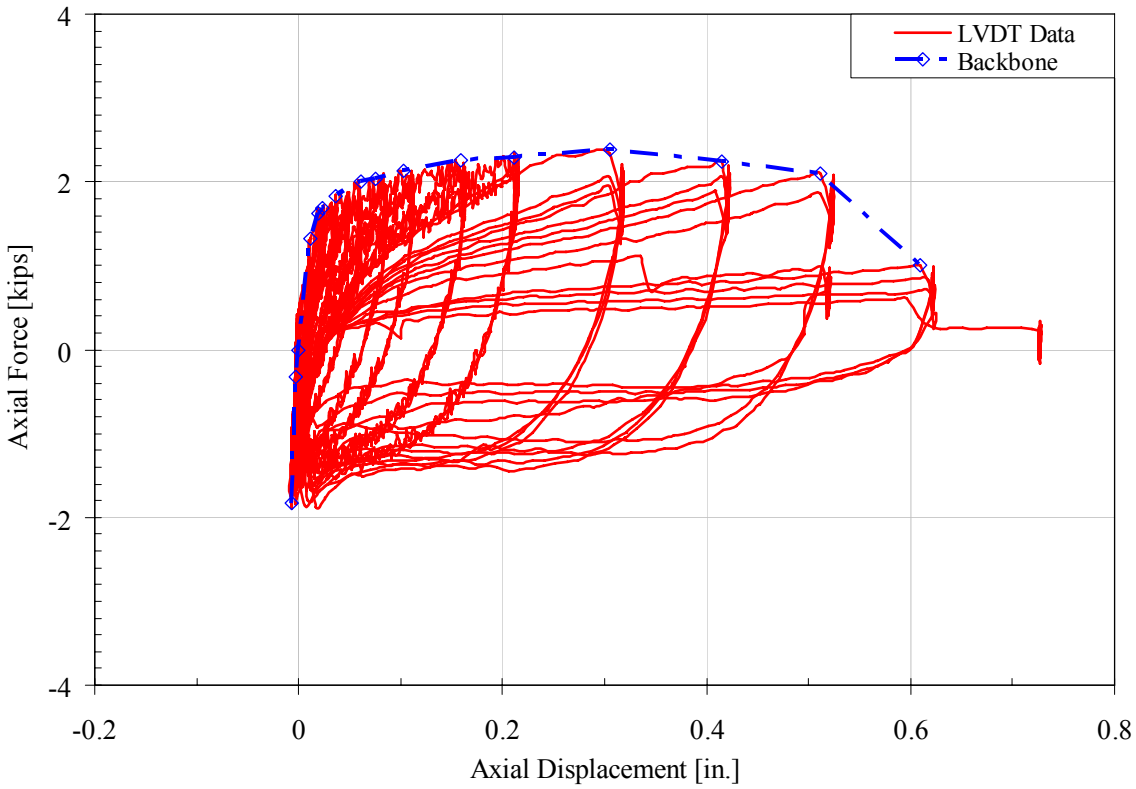

Figure 5-5: Axial Force and Axial Displacement for JVI Half Scale Connector O-1

5.2.1 Comparison between Full Scale and Half Scale

The half scale specimen response compares well with previous full scale test results. The results from the half scale tests were scaled to full scale by multiplying the displacements by 2.0 and forces by 4.0 in accordance with principals of similitude. The scaled test data is compared with results previously generated in ATLSS report 07-04[7]. The test protocol is identical to previous full scale JVI connector cyclic tension test carried out in Phase 1B test series.

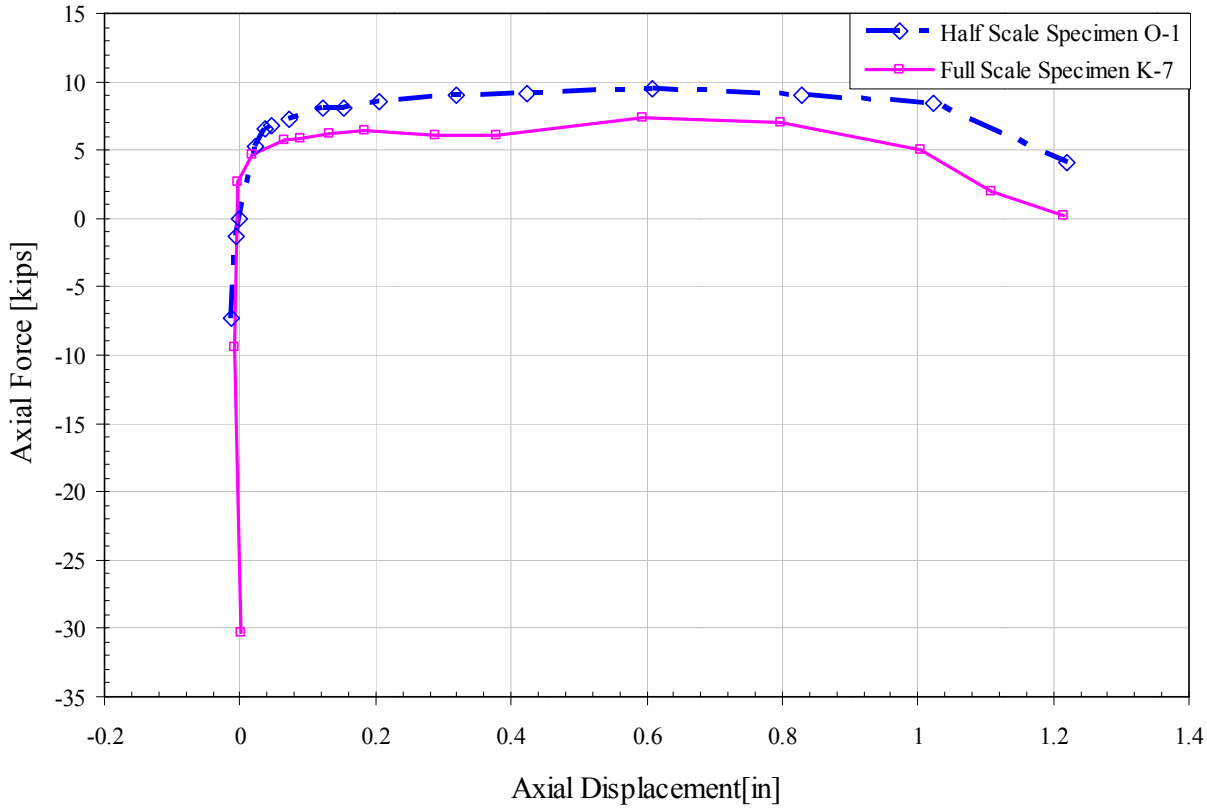

Figure 5-6: Cyclic Tension Envelopes of Half Scale and Full Scale JVI Connection

As shown in Figure 5-6, the tension force capacity of half scale test was higher than that of full scale test. The tensile deformation capacity of half scale tests was 1.2-in tensile opening, which is identical to the result of full scale test performed at Lehigh and summarized in ATLSS Report 07-04[7]. Both connectors failed due to the low cycle fatigue of the connector legs, the failure modes are displayed in Figure 5-7.

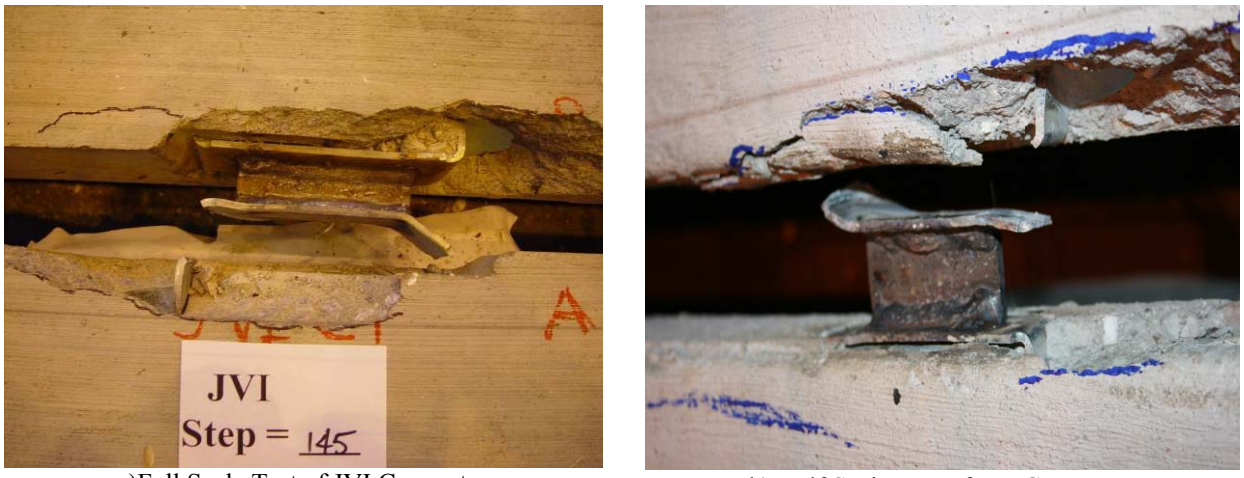

a)Full Scale Test of JVI Connector

b) Half Scale Test of JVI Connector

Figure 5-7: Failure Modes of Half Scale and Full Scale Cyclic Tension Test of JVI Connection

5.3. Type O-2: Half Scale JVI Cyclic Shear with ΔT=0

The performance of the Half Scale JVI Vector Connector subjected to cyclic shear is presented in this section. The panel was subjected to a cyclic shear displacement with the tensile displacement restrained, ΔT=0. A reference shear deformation of 0.0805 was used for the test, this value was based on the effective shear yield deformation of the half scale JVI connector, which was computed as half of the intercept of a horizontal line at the max load and a secant stiffness line at 75% of the max load of the full scale JVI connector under the monotonic shear loading protocol. Damage initiated with concrete cracking around connector on panel A., which resulted in a significant decrease in the capacity (see Figure 5-8 part a).This was followed by crack propagation and spalling around the connectors. After that, the left leg of the connector in Panel A began to crack and eventually fractured. Shortly afterwards, the right leg of the connector in Panel A fractured ending the test. The observed key events and the corresponding displacement level are presented in Table 5-4. The photos of the damage are presented in Figure 5-8. The global force deformation response and backbone curve are presented in Table 5-5, Figure 5-9 and Figure 5-10.

a) 0.041-in.

b) 0.243-in.

c) 0.486-in. - End of Test

Figure 5-8: Damage state at various shear deformations.

Table 5-4: Key Test Observations (Cyclic Shear with Axial Displacement = 0)

Event #	Shear Δ Step [in.]	Event Description
1	+0.010	Minor cracking on panel A top right hand side

Table 5-4: Key Test Observations (Cyclic Shear with Axial Displacement = 0)		
2	+0.061	Minor crack on panel A over left hand side around connector
3	+0.081	Cracks on panel A extended, small gap formed between the faceplate and Panel A
4	+0.122	Concrete around connector on Panel A spalled
5	+0.162	Concrete continued spalling
6	-0.162	Continued spalling
7	+0.243	fracture of left leg of connection(from top)
8	-0.243	fracture of right leg of connection(from bottom)
9	+0.324	Complete fracture of left leg of connector in Panel A
10	+0.486	Complete fracture of right leg of connector in Panel A. **End of test**

Table 5-5: Experimental Results Backbone Curve (Cyclic Shear with Axial Force = 0)		
Event	Shear Displacement [in.]	Shear Force [kips]
-	-0.485	-0.312
- Further propagation of cracks on the connector	-0.324	-0.591
- Fracture of right leg of connection(from bottom)	-0.243	-1.432
- Noise heard, Concrete continue spalled	-0.154	-2.155
-	-0.100	-3.019
-	-0.059	-4.016
-	-0.043	-4.901
-	0.000	0.000
-	0.031	4.257
- Peak load	0.047	5.450
- Minor crack on panel A over left hand side around connector	0.068	4.229
-	0.108	3.019
	0.144	1.974
	0.216	1.239
- Fracture of left leg of connection(from top)	0.225	0.698
	0.292	0.122
-Connector failed. End of test	0.452	0.004

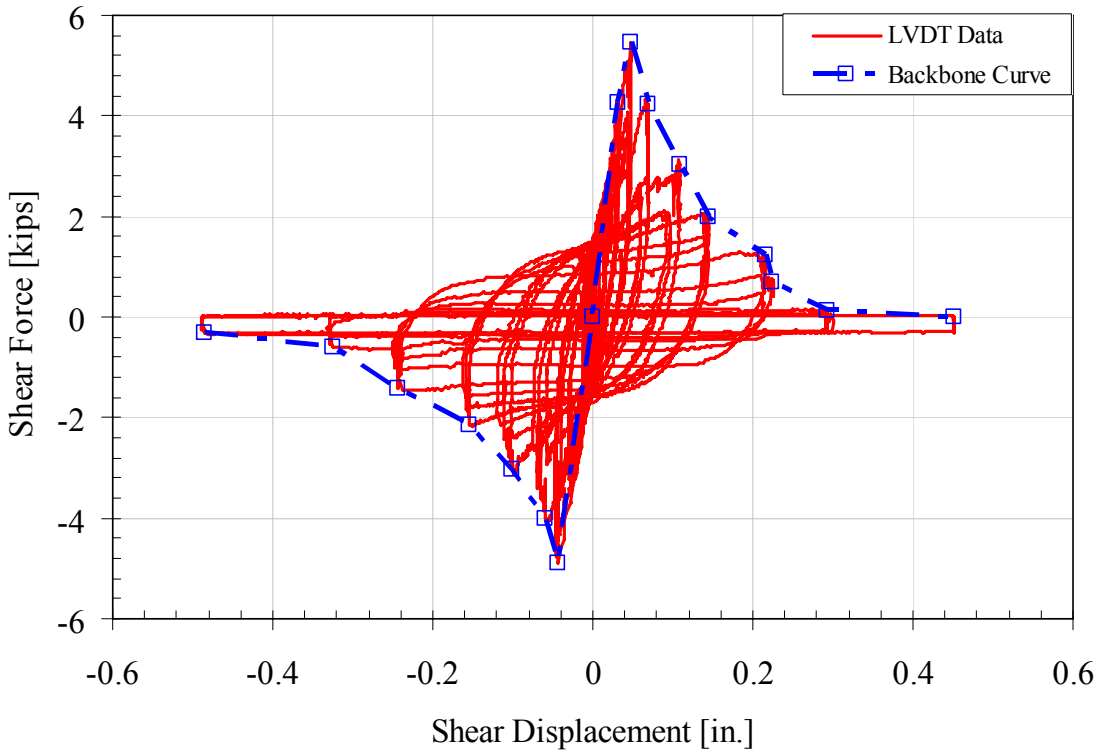

Figure 5-9: Shear Force and shear displacement for JVI Half Scale Connector

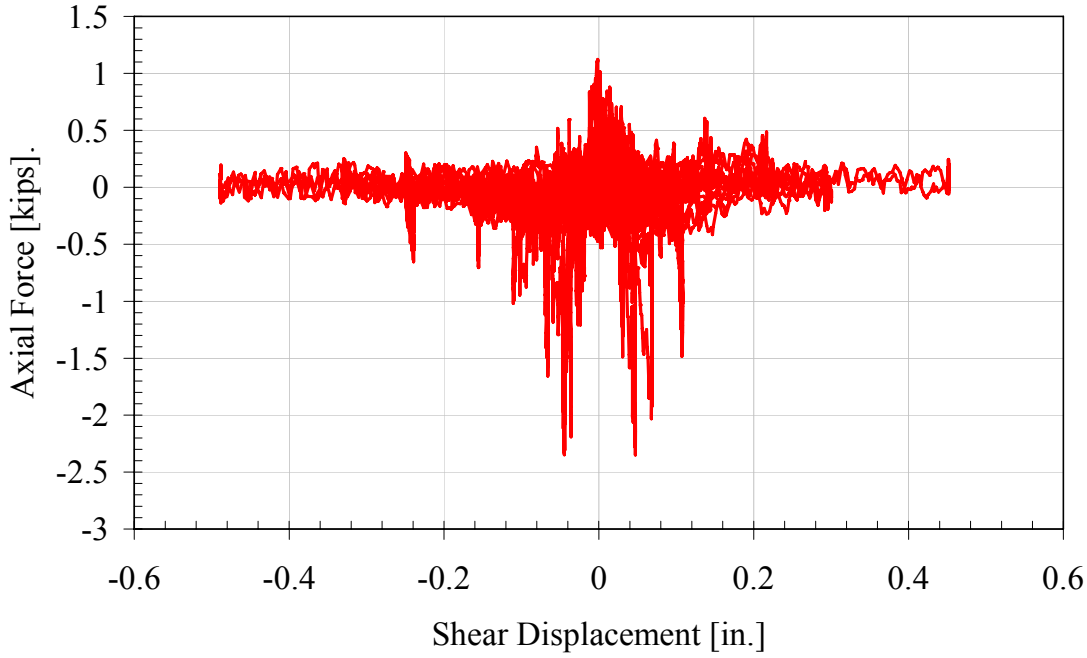

Figure 5-10: Axial force and shear displacement for JVI Half Scale Connector

5.3.1 Comparison between Full Scale and Half Scale

The half scale specimen response compares well with previous full scale test results. The peak load resistance and the corresponding deformation level at which it occurred were bounded by the full scale test results from tests K-1 and K-2. The drop in strength from peak was attributed to concrete crushing and cracking around the faceplate. The

unloading was similar to the full scale with a marginally steeper decrease in strength. This may be attributed to the aggregate size in the half scale test. Since the aggregate was not scaled the pieces were larger relative to the connector faceplate. This may have resulted in quicker loss of concrete around the connector after the peak strength was achieved. The deformation capacity was higher for the half scale test. The results from the half scale tests were scaled to full scale by multiplying the displacements by 2.0 and forces by 4.0 in accordance with principals of similitude. The scaled test data is compared with results of full scale test previously conducted. The test protocol was identical to previous full scale JVI connector cyclic shear test carried out in Phase 1B.

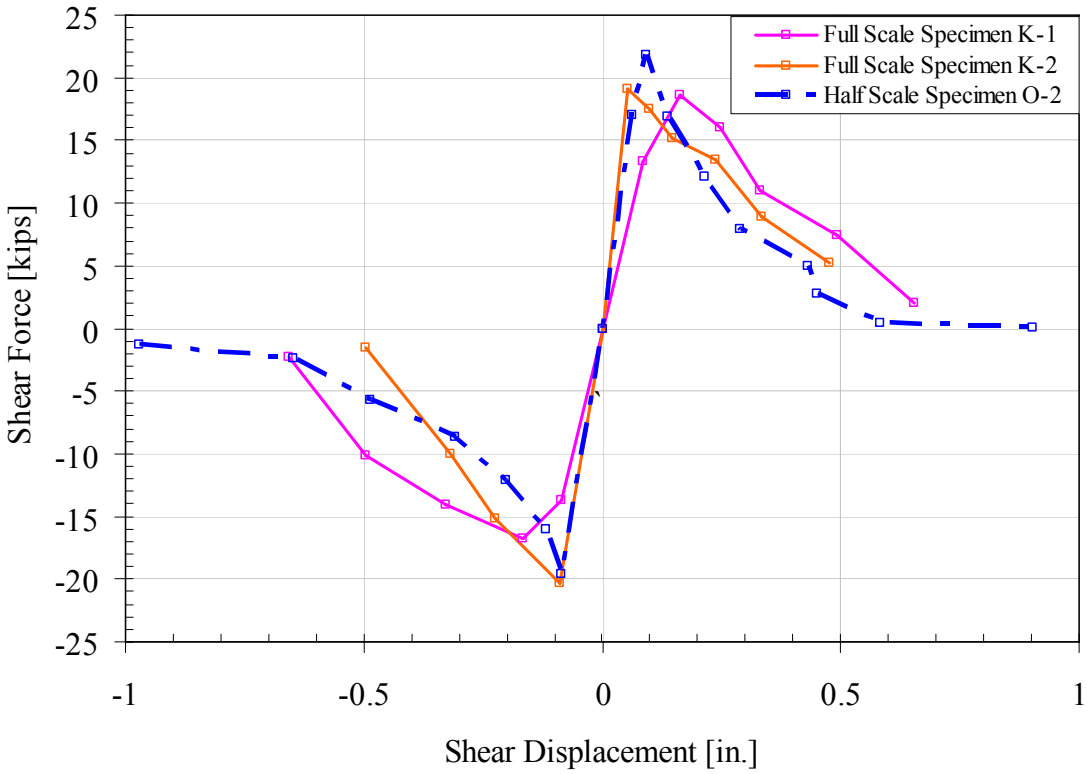

Figure 5-11: Cyclic Shear Envelopes of Half Scale and Full Scale JVI Connections

The connector failed by low cycle fatigue of the legs. The two cyclic shear full scale tests completed in phase 1B, had a measured shear capacity of 19.05-kips and 18.65-kips respectively. Comparatively, the shear force capacity of half scale test was higher than that of full scale test. The shear deformation capacity of the half scale and full scale tests compared well with each other at about 0.60 in. The failure modes are displayed in Figure 5-12.

a)Full Scale Test of JVI Connector

b) Half Scale Test of JVI Connector

Figure 5-12: Failure Modes of Half Scale and Full Scale Cyclic Shear Test of JVI Connection

5.4. Summary about Comparison between Full Scale and Half Scale

As indicated in this section, for both cyclic tension and cyclic shear test of JVI connectors, the scaling did significantly affect the response or failure modes of the connector. The force capacity of half scale tests are slightly higher than that of full scale tests, and the deformation capacity of half scale tests are comparable with the full scale tests, it is reasonable to use the data of half scale tests with proper factor to represent behavior of full scale tests.

6. TYPE P: HALF SCALE TOPPED HAIRPIN WITH DUCTILE MESH

The Ductile Ladder Connector was developed in coordination with Ivy Steel and Wire, Inc. The connector was fabricated from 1018 wire which has not been subject to the cold-rolling process. The welds were conducted at room temperature using a robotic welding process according to AWS specifications and ASTM standards. It is worth mentioning that the Ductile Ladder connector is a kind of special Welded wire reinforcement (WWR), since the conventional WWR is required using cold-drawn wires according to the ASTM A82 and A185. Without the cold-drawn process, the Ductile Ladder connector has a much higher ductility. The measured elongation of the wire is typically about 30%. If strain occurs over the entire length between cross-wires, this elongation capacity would produce an axial deformation capacity of 3-in. across the 10-in. length of the ladder cross-members. The connector has the potential to possess a high axial capacity and deformation capacity. The "ladder" wire configuration would act as a series of springs to resist the forces imposed on the diaphragm under moderate to large joint openings. The expected failure mode is fracture of the wires across the panel joint.

This ductile mesh connection was used in conjunction with a low cost "hairpin" connection fabricated from a bent #2 A706 reinforcing bar which was chosen to represent a half scale of the typical hairpin connector made by #4 A706 reinforcing bar. The specimen consists of a 1.5-in field placed topping used over a double tee with at 1 in. thick flange. The specimen represents a half scale of a 2-in. precast concrete flange with a 3-in field placed topping. The topping thickness is larger than the typical construction of a 2-in. cast-in-place top. The larger thickness was chosen to match specimens constructed at UCSD.

The 10x12 W4.9xW4.9 ductile mesh used in Phase 1B test series was fabricated from hot formed wire. The 0.049 in^2 cross section of the W4.9 wire is the smallest size hot-rolled 1018 wire produced in the United States. Smaller sizes are fabricated by the cold rolling process which significantly decreases the ductility of the wire. Consequently, the size of ductile mesh was not modified.

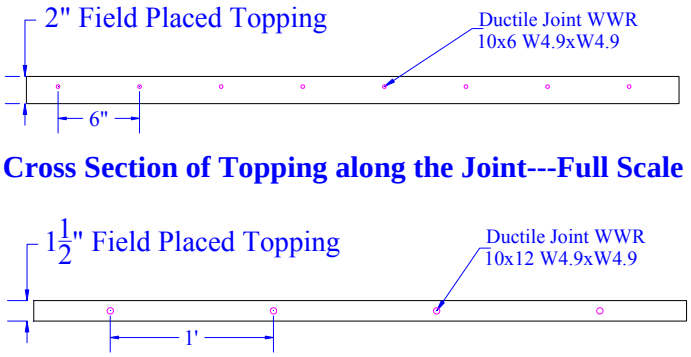

Figure 6-1: Cross Section of Topping along the Joint of Half Scale and Full Scale Specimens

However, the transverse wire spacing was increased from 6-in to 12-in as shown in Figure 6-1, which resulted in the decrease of area of wires crossed joint compared with the connectors summarized in ATLSS Report 07-04 [7]. As calculated in equation 6-1, the ratio of steel area to the gross area of concrete, ρ_f, for full scale specimen is around 0.0041, ρ_h, for half scale specimen is around 0.0027. So the resulting half scale specimen P-1 consists of a half scale hairpin connector and a same size ductile mesh connector with less amount(about half of the area of steel used previously) of steel crossing the joint.

$$\rho = \frac{A_{steel}}{A_{concrete}} \qquad 6\text{-}2$$

Details of the half scale topped hairpin and ductile mesh connection are illustrated in Figure 6-2 and Figure 6-3, as a comparison, details of the full scale topped hairpin and ductile mesh connection are illustrated in Figure 6-4.

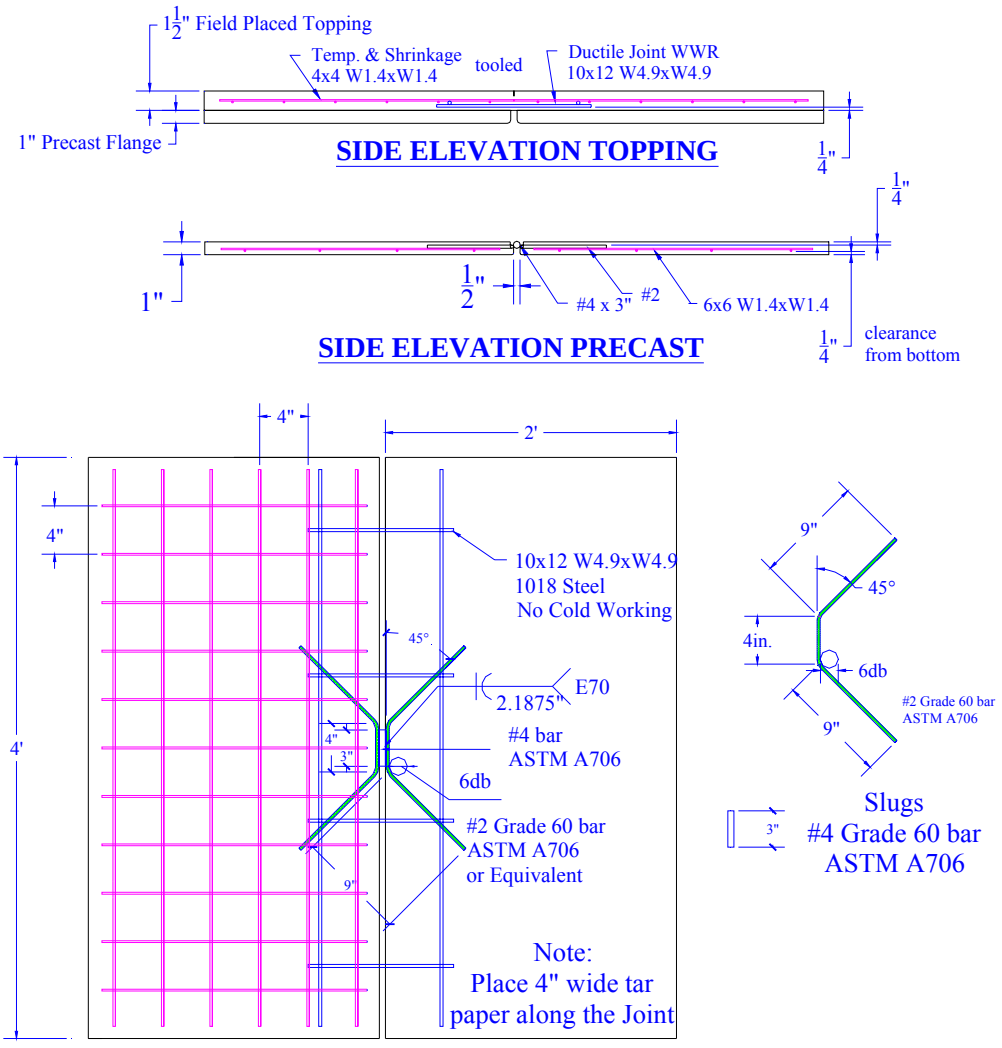

Figure 6-2: Half Scale Topped Hairpin & Ductile Mesh Connector Details (Type P)

Figure 6-3: Half scale Topped Hairpin & Ductile Mesh Connector

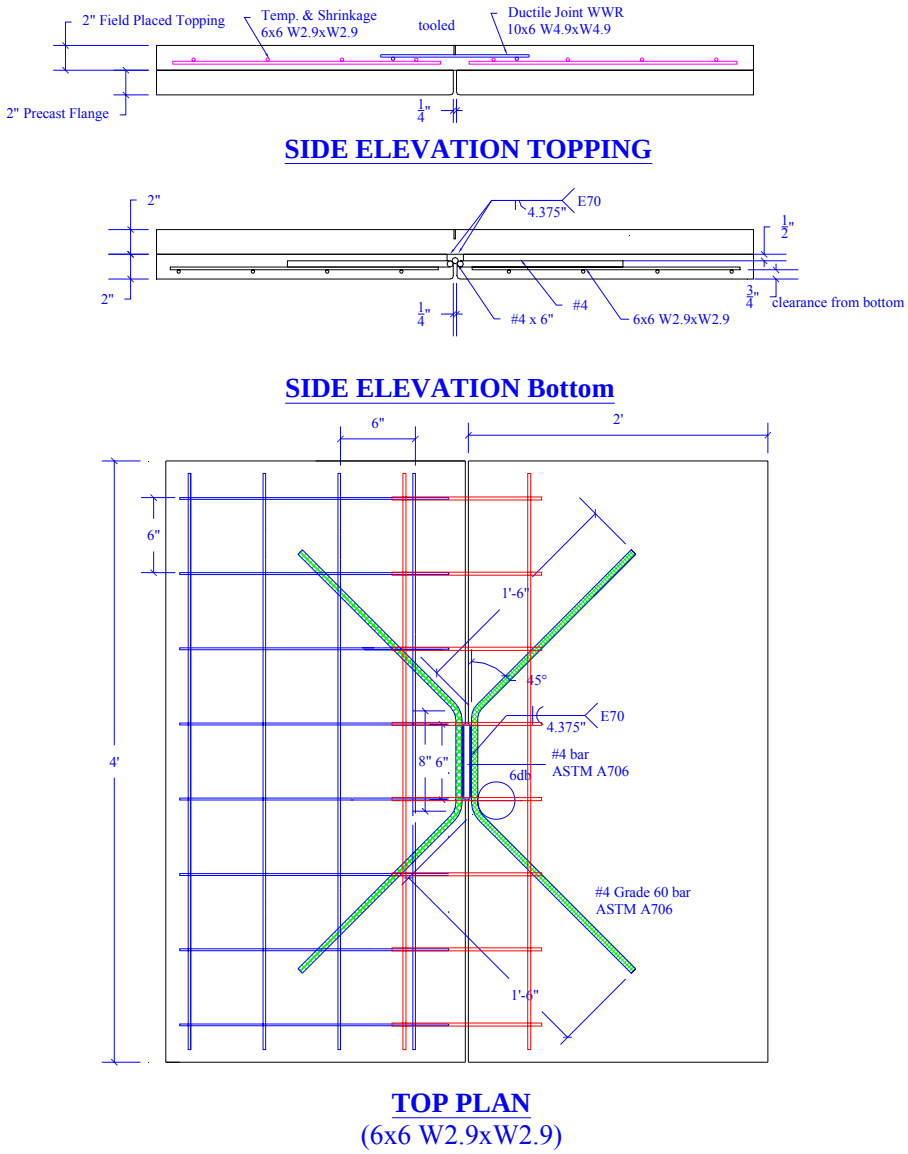

Figure 6-4: Full Scale Topped Hairpin & Ductile Mesh Connector (Type L)

6.1. Material Properties Topped Hairpin with Ductile Mesh

The 1-in. precast concrete panel was fabricated with design strength of 6000 psi, and the 1.5-in. filed topping was fabricated with design strength of 4000 psi. The compressive strength of the concrete when the panel tests were conducted was measured in accordance with ASTM C39. The temperature and shrinkage WWR used in the precast panel met the requirements of ASTM A185 grade 65 steel. The connector was fabricated from ASTM A706 grade 60 reinforcing bars. The measured concrete strengths and mill certified steel properties are presented in Table 6-1.

Table 6-1: Material Properties Capacity

Concrete Panel Type	Compressive Strength, f'c [psi]
Base Panel	7088 ±51
Topping	6803±123

Size	Reinforcement Usage	Grade	Yield Stress [ksi]	Ultimate Strength [ksi]
#2	Connector	A706	65.6	94.3
#4	Reinforcing Bars	A615 Gr. 60	67.7	105.4
4 X 4 W1.4XW1.4	Pre-cast Panel Mesh	A185 Gr. 65	65.00*	108.5
10 X 12 W4.9XW4.9	Ductile Ladder Connector	1018	54.2	76.6
* Data unavailable, value assumed				

6.2. Type P-1: Topped Hairpin with Ductile Mesh Cyclic Tension with Shear Force =0

The performance of the topped hairpin with ductile ladder connection subjected to cyclic tension and compression is presented in this section. The panel was subjected to axial displacement with the shear displacement unrestrained, Fv=0. A reference tension deformation of 0.05 was used for the test, this value was based on the effective tension yield deformation of the half scale topped hairpin with ductile mesh connector, which was computed as half of the intercept of a horizontal line at the max load and a secant stiffness line at 75% of the max load of the full scale topped hairpin with ductile mesh connector under the monotonic tension loading protocol. Panel damage initiated with the formation of a longitudinal crack in the topping above the joint in the panels. The center joint crack expanded and contracted during the cyclic demands without of incident until 0.5-in at which time one wire of ductile mesh fractured. As the displacement demands increased failure of the remaining ladder wires occurred. Failure of the legs of hairpin connector B occurred at 0.8 in. and severed the connection between the panels thus ending the test. Observed key events and the corresponding displacement level are presented in Table 6-2. The photos of the damage are presented in Figure 6-5 and Figure 6-6. The global force deformation response and backbone curve are presented in Table 6-3 and Figure 6-7.

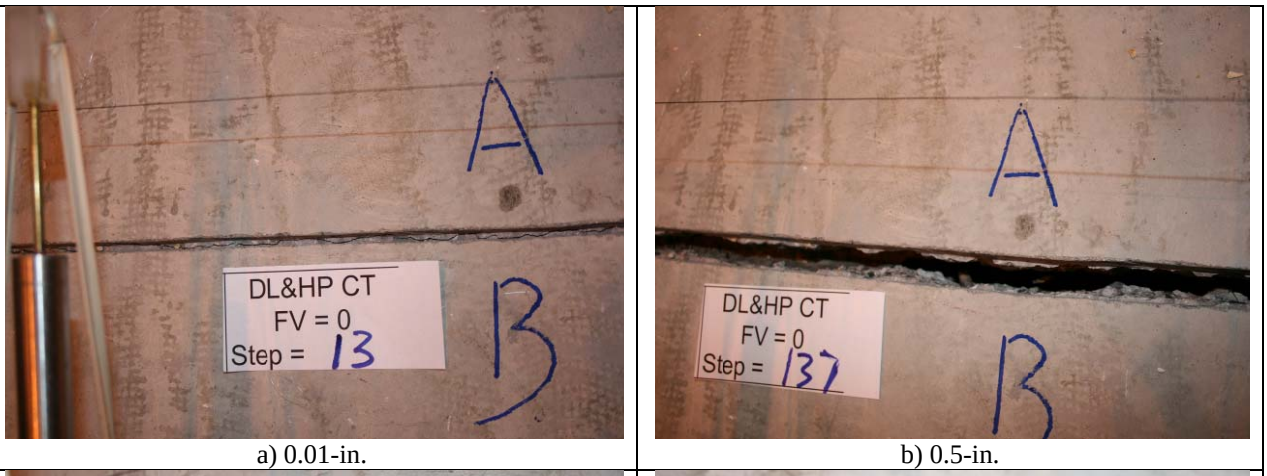

a) 0.01-in. b) 0.5-in.

c) 1.0-in. d) 1.6-in.

Figure 6-5: Damage state at various axial deformations.

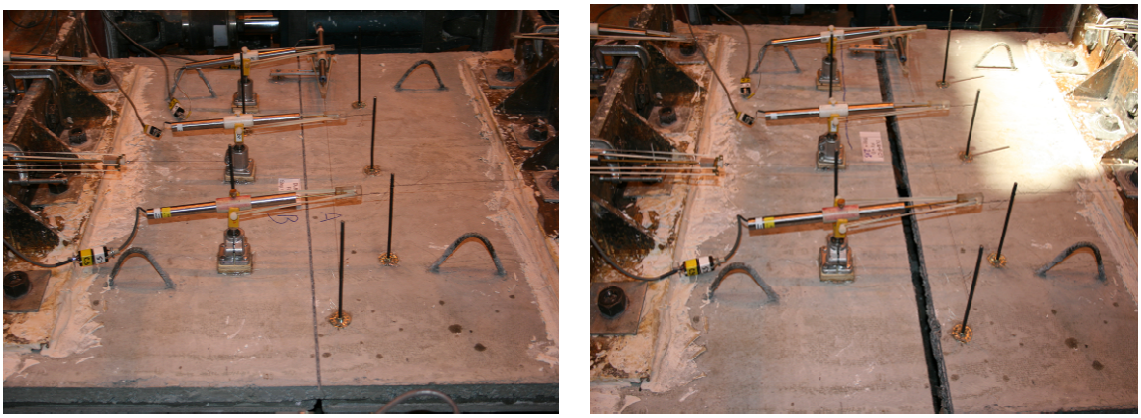

Figure 6-6: Initial and final overall condition

Table 6-2: Observed key events (Cyclic Tension)		
Event #	Tensile Δ [in.]	Event Description
1	0.0125	Center Cracked between panels
2	0.100	One horizontal crack over the left side of Panel B formed
3	0.150	Center crack open approximately 1/8", the horizontal crack extended
4	0.200	Center crack open approximately 1/4".
5	0.300	One small vertical crack occurred over the left side of panel B.
6	0.400	Center crack open approximately 1/2". Ductile ladder exposed in the center crack(4 bars)
7	0.500	Two wires of ductile mesh fractured
8	0.600	Two additional wires of ductile mesh fractured
9	0.700	Propagation of weld fracture
10	0.80	Legs of hairpin connector in Panel A fractured. **End of test.**

Table 6-3: Experimental Results Backbone Topped Hairpin Connector (Cyclic Tension)		
Event	Shear Displacement [in.]	Shear Force [kips]
-	0.010	-48.830
- Center Cracked between panels	0.010	-40.947
-	0.000	0.000
-	0.008	4.806
-	0.021	11.920
-	0.031	13.922
-	0.078	14.064
- One horizontal crack over the left side of Panel B formed	0.106	13.597
- Center crack open approximately 1/8", the horizontal crack extended	0.153	13.554
- Center crack open approximately 1/4.	0.202	13.773
- One small vertical crack occurred over the left side of panel B	0.301	14.687
- Peak Load; Center crack open approximately 1/2". Ductile ladder exposed in the center crack(4 bars)	0.400	14.869
- Two wires of ductile mesh fractured	0.501	10.997
- Two more wires of ductile mesh fractured	0.598	4.082
- Welds continuing to fracture	0.698	1.956
- Legs of hairpin connector in Panel A fractured. **End of test.**	0.803	0.295

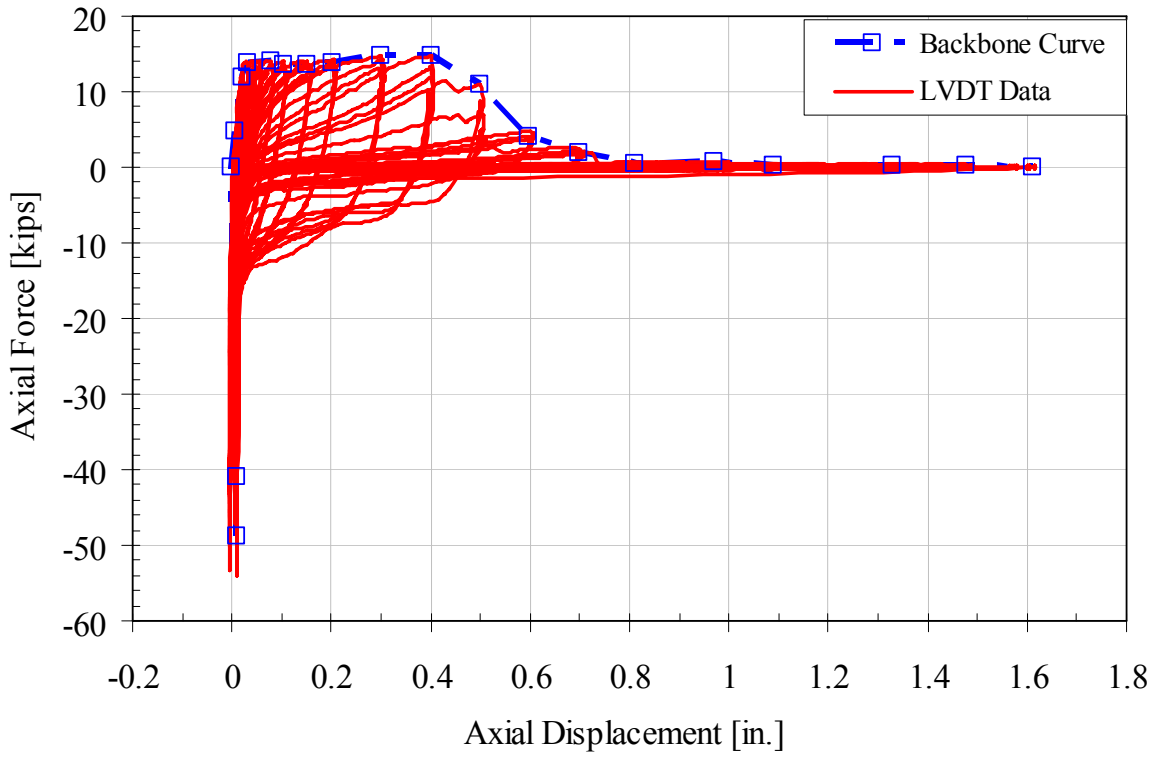

Figure 6-7: Axial Force and Axial Displacement for Half Scale Topped Hairpin with Ductile Mesh Connector

6.2.1 Comparison between Full Scale and Half Scale

The results of the half scale specimen P-1 were scaled to full scale by multiplying the displacements by 2.0 and forces by 4.0 and then the scaled test data is compared with results of full scale topped hairpin with ductile mesh specimen L-1 tested in Phase 1B and summarized in ATLSS Report 07-04[7]. However, as indicated at the beginning of Section 6. , the half scale specimen P-1 of topped hairpin with ductile mesh connector consisted of a half scale hairpin connector and a ductile mesh connector with half area of steel crossing the joint, while the full scale specimen L-1 was fabricated with a full scale hairpin connector and ductile mesh connector. It is expected that this comparison will result in a higher capacity estimation of half scale test as shown in Figure 6-8.

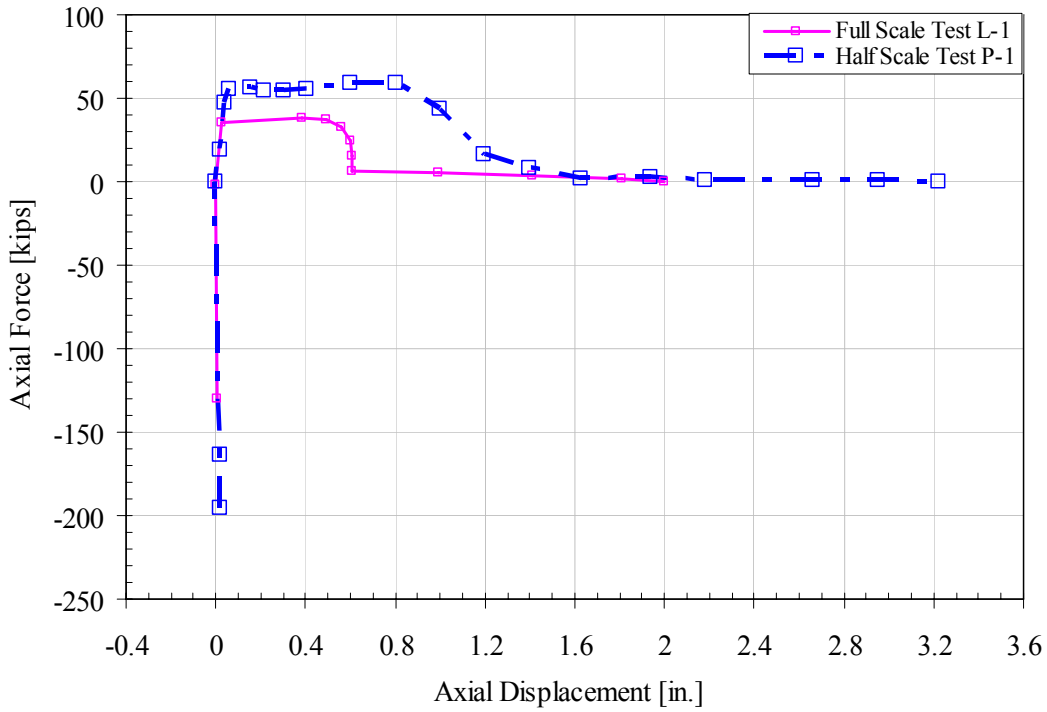

Figure 6-8: Cyclic Tension Envelops of Half Scale Specimen P-1 and Full Scale Specimen L-1

As previously indicated, the half scale topped hairpin with ductile mesh specimen P-1, of which the hairpin connector was fabricated at a half scale, while the ductile mesh connector was examined at full scale but the area of steel crossed joint was about half of which used previously. In order to get a more accurate comparison between the half scale and full-scale connectors, the full-scale bare untopped hairpin data combined with the full-scale bare ductile mesh data were chosen to compare with the results of half scale specimen P-1. The untopped hairpin specimen C-1 was tested in Phase 1A and is summarized in ATLSS report 06-03[8] and it is worth to point out that the specimen C-1 was tested under the monotonic loading, the results were still used since the cyclic test results are not available for the untopped hairpin connector. The ductile mesh specimen H-6 was tested in Phase 1B and is summarized in ATLSS Report 07-04 [7]. The behavior of specimen C-1 and specimen H-6 is displayed in Figure 6-9.

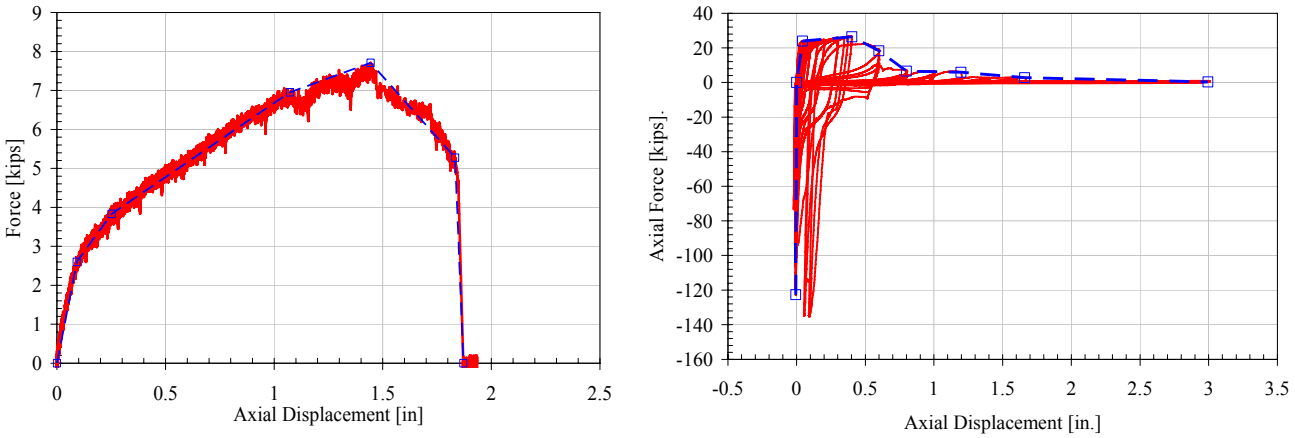

a) Tensile force and displacement of Specimen C-1 b) Tensile force and displacement of Specimen H-6

Figure 6-9: Tensile Force and Displacement of specimen C-1 and Specimen H-6

Since it is not possible to separate the hairpin and ductile mesh behavior in specimen P-1, it is necessary to scale the full scale results to half scale for this comparison, instead of scaling the half scale to full scale as conducted in previous comparison. To compare the results a scale factor of 0.25 was used for bare hairpin full scale test tensile force data and a factor of 0.5 was used for tension deformation data of specimen C-1, similarly, a scale factor of 0.5 was used for bare ductile mesh full scale test tensile force data and a length scale factor of 1 was used for tension deformation data of specimen H-6, the summation of the results of specimen C-1 and specimen H-6 was used to compare with the original data of half scale specimen P-1, the connector behavior is displayed in Figure 6-10:

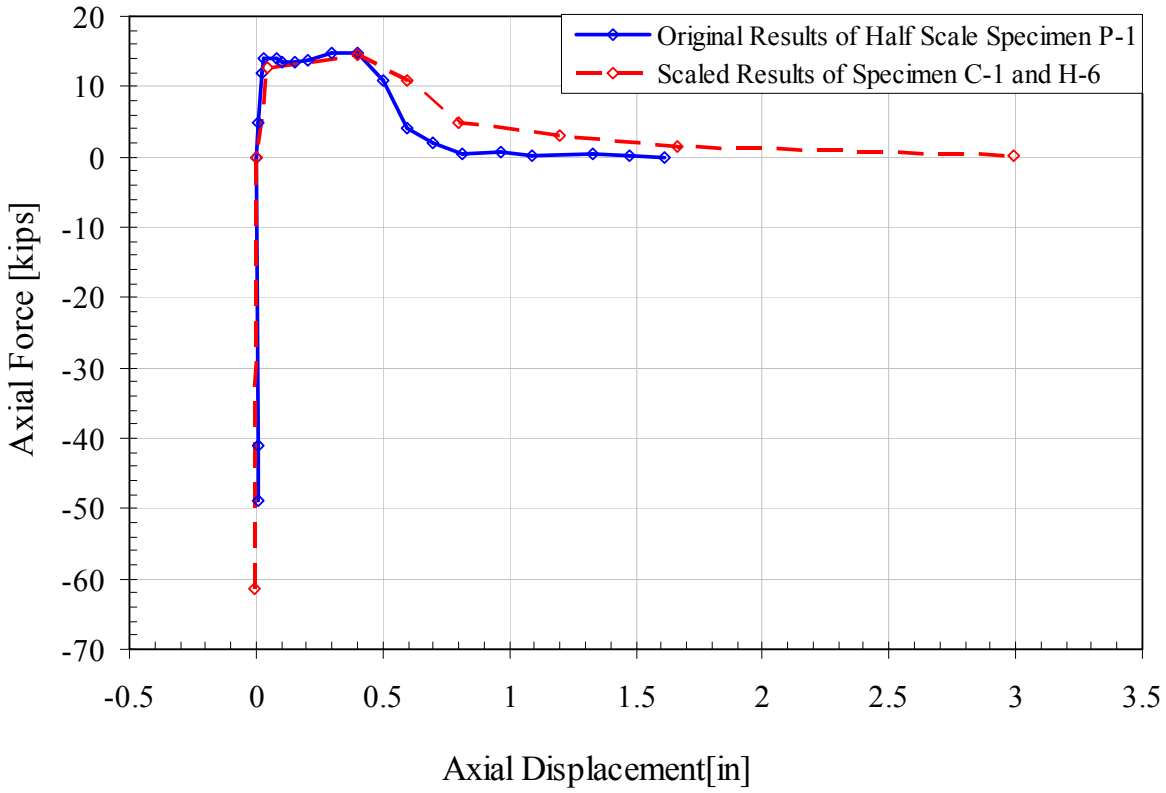

Figure 6-10: Cyclic Tension envelope comparison of specimen P-1 and scaled behavior of specimens C-1 and H-6

As illustrated in Figure 6-10, the half scale specimen P-1 response compares well with scaled results of previous full scale specimen C-1 and H-6. They both yielded at a same tensile opening of 0.03-in and had a similar force capacity of 14.60-kips. Also, they had a significant decrease in capacity at the same tensile opening of 0.4-in but the rate of decrease of force capacity of specimen P-1 is higher than the combined full-scale test response. The decrease in strength was associated with the cracking and crushing of the concrete. The rapid decrease in strength may be due to the fact that the aggregate was not scaled. The larger relative aggregate size may have resulted in a quicker loss of load carrying capacity.

It was predicted that specimens would have a much higher displacement capacity since the ductile mesh is fabricated with hot-rolled 1018 wire which has an approximate fracture strain of 30%. The measured displacement capacity of the topped hairpin and ductile mesh connector, however, was limited to approximately 0.4-in. This phenomenon also occurred for the bare ductile mesh connector specimen H-6 test as illustrated in Figure 6-9 b. It is concluded that the ductile mesh failed early and could not get the expected high ductility, which may be due to low cycle fatigue of hot –rolled 1018 steel or due to the fact that the strain in the wire occurred over a length much shorter than the overall wire length.

The premature failure of the ductile mesh can likely be attributed to either low-cycle fatigue or the fact that the strain in the wire occurred over a length much shorter than the overall wire length. The ductile mesh was subject to 73 cycles prior to fracture. Research by Amorn et al [9] has showed that conventional cold-rolled WWR will fail in high cycle fatigue, however, the ductile mesh was fabricated from hot-rolled material and it may be subject to low-cycle fatigue concerns. Research by Plumtree et al [10] has shown that 1018 steel will soften under cyclic loading even under low stress cycles. Combining this with a potential shorter strain length may have resulted in higher stress cycles on the mesh crossing the joint and the premature fracture. To validate this hypothesis would require additional material testing.

The failure modes of specimen P-1 is compared with specimens L-1 in Figure 6-11. The cyclic axial motion of both tests resulted in the failure of the ductile ladder followed by the topped hairpin. For the full scale test, the test ended with fracture of the slug to hairpin weld, while the half scale ended with fracture of legs of hairpin connector. The difference between the two modes of failure is likely due to a larger weld in the half-scale tests. Due to the size of the #2 bar it is difficult to deposit the exact amount of weld metal. The size was likely larger than the amount used on the full-scale test. This may have resulted in the change in the failure mode observed.

a)Full Scale Test b) Half Scale Test

Figure 6-11: Failure Modes of Half and Full Scale Cyclic Tension Test of Topped Hairpin with Ductile Mesh Connector

6.3. Type P-2: Topped Hairpin w/ Ductile Mesh Cyclic Shear with ΔT = 0.05-in

The performance of the topped hairpin with ductile ladder connection subjected to cyclic shear is presented in this section. The panel was subjected to shear displacement with the tensile displacement kept constant at an opening of ΔT= 0.05-in. A reference shear deformation of 0.133 was used for the test, this value was based on the effective shear yield deformation of the half scale topped hairpin with ductile mesh connector, which was computed as half of the intercept of a horizontal line at the max load and a secant stiffness line at 75% of the max load of the full scale topped hairpin with ductile mesh connector under the monotonic shear loading protocol. Connector damage was initiated with a concrete cracking around the connector of panel B formed when applying the initial tension displacement 0.05-in. Concrete spalled at 0.20-in. The test ended at 2.93-in. with audible bar fracture of the hairpin connector. The observed key events and the corresponding displacement level are presented in Table 6-4. Photos of the damage at various deformations and initial and final conditions are presented in Figure 6-12 and Figure 6-13 respectively. The global force deformation response and backbone and envelope curves are presented in Table 6-5, Figure 6-14, and Figure 6-15.

a) 0.05-in.

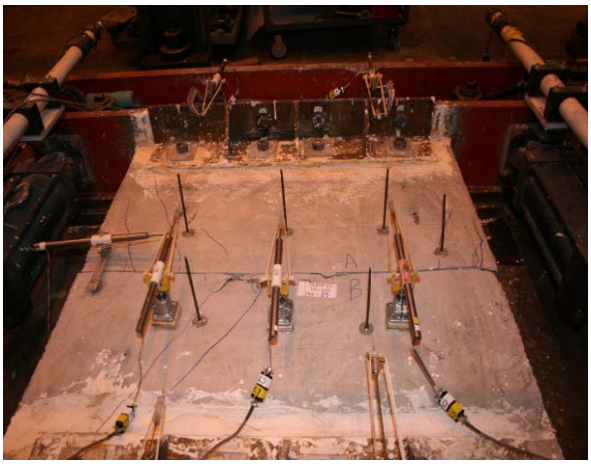

b) -0.40-in.

c) 1.60-in.

d) -2.90-in.(visible hairpin damage)

Figure 6-12: Damage state at various shear deformations.

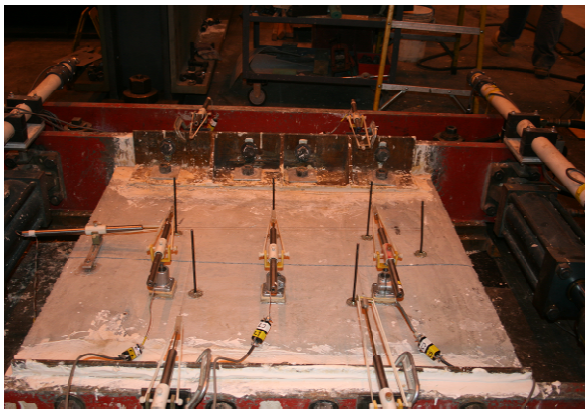

Figure 6-13: Initial and final overall condition

Table 6-4: Observed key events (Cyclic Shear)		
Event #	Shear Δ Step [in.]	Event Description
1	0.05(T)	Crack around the connector of Panel B
2	0.399	Two diagonal cracks formed on Panel B to the support
3	-0.399	Three diagonal cracks formed on Panel A to the support, Audible popping
4	0.532	Spalling on Panel B over the cracked area.

Table 6-4: Observed key events (Cyclic Shear)		
5	-0.532	Noise heard, Spalling on Panel A
6	0.798	Additional spalling on both panels, moved the LVDT 8 holder because of the spalling of concrete over the area
7	2.394	Noise heard, Additional spalling
8	2.926	Ductile mesh strand fractured(Visible at this step)
9	3.458	Two more ductile mesh strands and one leg of hairpin fractured (visible at this step).
10	3.990	Shear LVDT out of range in positive direction
11	4.256	All the strands fractured(Visible at this step)

Table 6-5: Experimental Results Backbone Topped Hairpin Connector (Cyclic Shear)		
Event	Shear Displacement [in.]	Shear Force [kips]
-	-2.920	-3.807
-	-2.655	-5.776
- Additional spalling	-2.390	-6.296
- Additional spalling	-2.125	-6.690
- Additional spalling	-1.854	-7.678
-	-1.594	-8.246
-	-1.606	-10.339
- Additional spalling	-0.798	-12.885
- Noise heard, Spalling on Panel A	-0.531	-17.627
- Three diagonal cracks formed on Panel A to the support	-0.398	-46.029
-	-0.266	-40.459
-	-0.233	-38.289
-	0.000	0.000
- Vertical Crack on the right corner of Panel A extended and one more vertical crack formed over there	0.195	31.151
- Peak Load, Two diagonal cracks formed on Panel B to the support	0.396	42.549
- Additional spalling on Panel B	0.529	14.400
- Additional spalling on both panels; removed the LVDT 8 due to spalling of concrete.	0.795	10.717
- Additional spalling	1.060	9.505
-	1.325	7.192
- Additional spalling.	1.591	9.245
- Additional spalling	1.856	7.007
- Additional spalling	2.123	6.590
- Additional spalling	2.388	7.353
- Fracture audible	2.653	5.990
	2.919	2.904

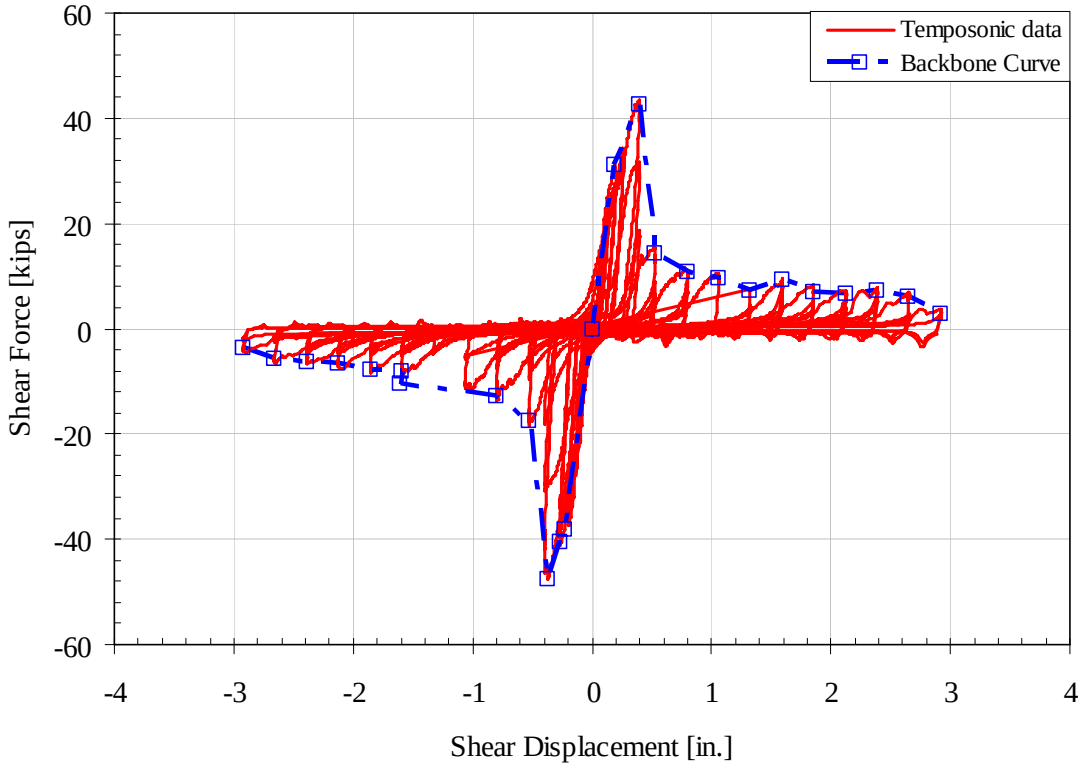

Figure 6-14: Shear force and shear displacement for half scale topped hairpin with ductile mesh connector

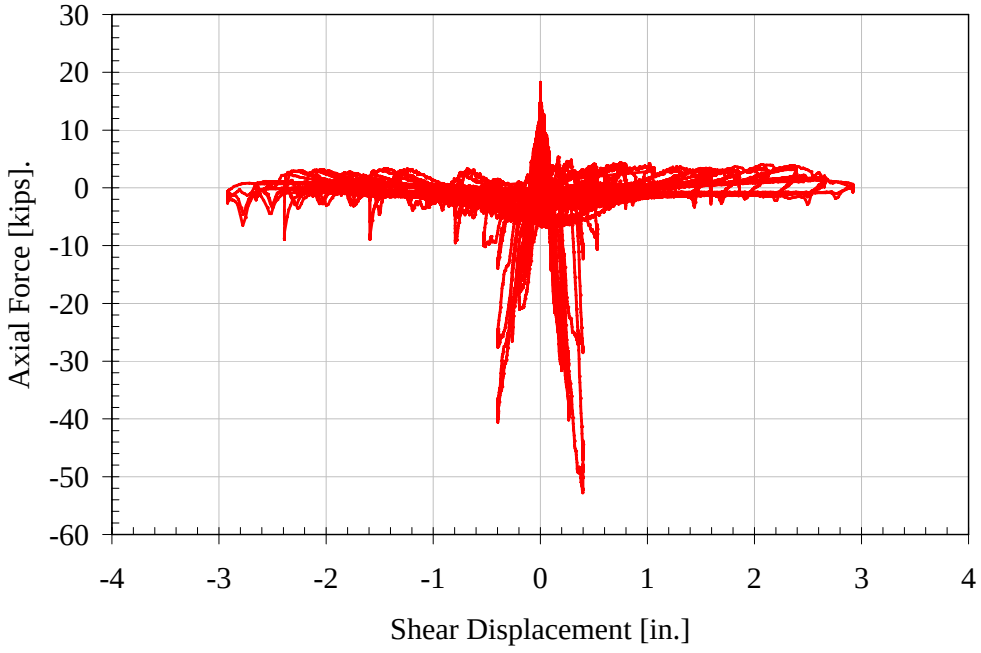

Figure 6-15: Axial force and shear displacement for half scale topped hairpin with ductile mesh connector

6.3.1 Comparison between Full Scale and Half Scale

The results of the half scale specimen P-2 were scaled to full scale by multiplying the displacements by 2.0 and forces by 4.0 and then the scaled test data is compared with results of full scale topped hairpin with ductile mesh specimen L-2 tested in Phase 1B and summarized in ATLSS Report 07-04[7]. However, as indicated at the beginning of Section 6. , the half scale specimen P-2 of topped hairpin with ductile mesh connector consisted of a half scale hairpin connector and a ductile mesh connector with half area of steel crossing the joint, while the full scale specimen L-2 was fabricated with a full scale hairpin connector and ductile mesh connector. Thus the half scale provides a much higher estimation of the capacity as shown in Figure 6-16.

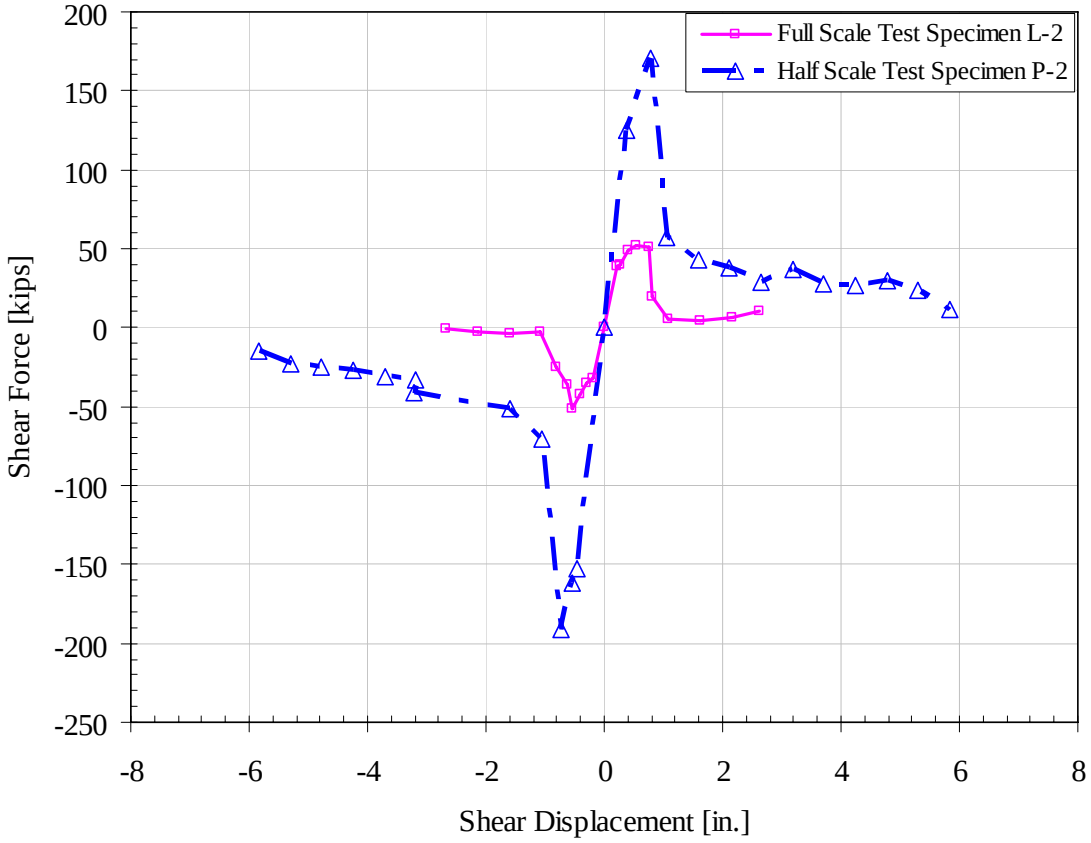

Figure 6-16: Cyclic Shear Envelops of Half Scale Specimen P-2 and Full Scale Specimen L-2

As previously indicated, the half scale topped hairpin with ductile mesh specimen P-2, of which the hairpin connector was fabricated at a half scale, while the ductile mesh connector was examined at full scale but the area of steel crossed joint was about half of which used previously. In order to get a more accurate comparison between the half scale and full-scale connectors, the full-scale bare untopped hairpin data and the full-scale bare ductile mesh data were combined and compared with the scaled results of half scale specimen P-2. The untopped hairpin specimen C-2 was tested in Phase 1A and is summarized in ATLSS report 06-03[8]. The ductile mesh specimen H-5 was tested in Phase 1B and is summarized in ATLSS Report 07-04 [7]. The behavior of specimen C-2 and specimen H-5 is displayed in Figure 6-19.

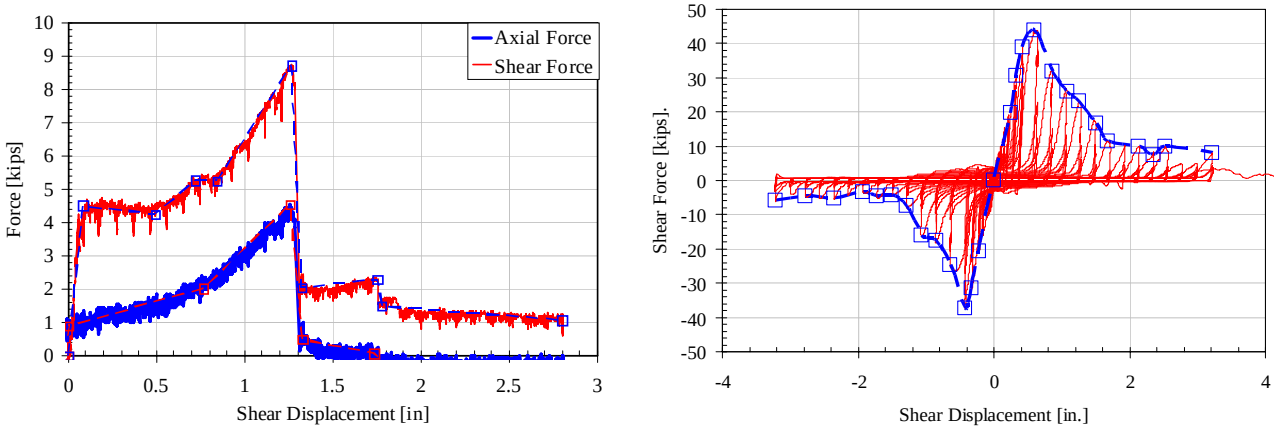

a) Shear force and displacement of Specimen C-2

b) Tensile force and displacement of Specimen H-5

Figure 6-17: Tensile Force and Displacement of specimen C-2 and Specimen H-5

Since it is not possible to separate the hairpin and ductile mesh behavior in specimen P-2, it is necessary to scale the full scale results to half scale for this comparison, instead of scaling the half scale to full scale as conducted in previous comparison. To compare the results a scale factor of 0.25 was used for bare hairpin full scale test shear force data and a factor of 0.5 was used for shear deformation data of specimen C-2, similarly, a scale factor of 0.5 was used for bare ductile mesh full scale test shear force data and a length scale factor of 1 was used for shear deformation data of specimen H-5, the summation of the results of specimen C-2 and specimen H-5 was used to compare with the original data of half scale specimen P-2, the connector behavior is displayed in Figure 6-18:

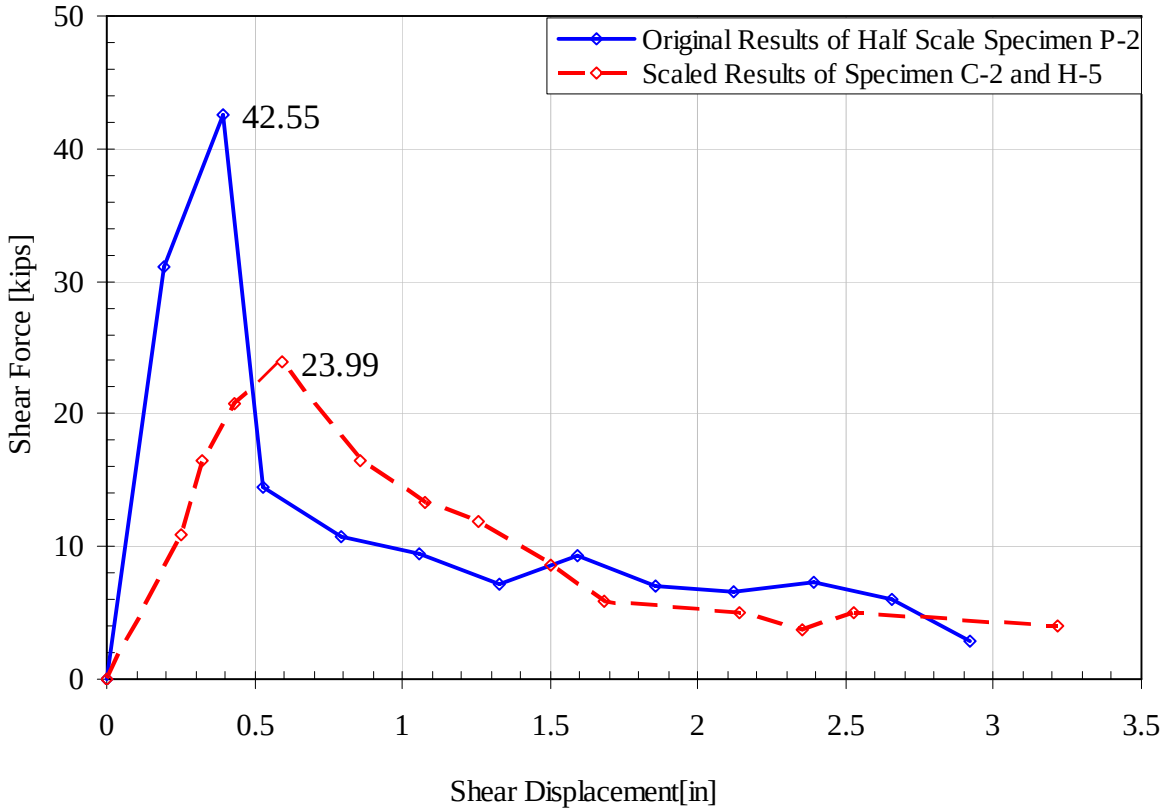

Figure 6-18: Cyclic shear envelope comparison of specimen P-2 and scaled behavior of specimens C-2 and H-5

As illustrated in Figure 6-18, similar to the tension test, both the half scale specimen P-2 response and scaled results of previous full scale specimen C-2 and H-5 had a significant decrease in capacity after the peak load, but the rate of decrease of force capacity of specimen P-2 is higher than the combined full-scale test response. The decrease in strength was associated with the cracking and crushing of the concrete. The rapid decrease in strength may be due to the fact that the aggregate was not scaled. The larger relative aggregate size may have resulted in a quicker loss of load carrying capacity. Also, the half scale specimen P-2 had a much higher force capacity with a lower shear deformation capacity then the scaled results of previous full scale specimen C-2 and H-5, which may be due to the difference of loading conditions for the half scale and full scale tests.

Based on the conditions and availability of data of previous tests, instead of comparing the full scale and half scale test directly, the original results of both tests are compared to the analytical force capacity according to ACI design standards [1]. The results of cyclic shear test of bare ductile mesh connector were also included for performance comparison. The connector performance is displayed in Figure 6-19.

The related ACI design equations are summarized in the Table 6-6. The first equation is the general shear friction model with the frictional contribution of the concrete included in the μ factor. The second equation (ACI 318 C11.6) gives more detailed calculations for the concrete contribution to the shear friction. The shear friction coefficient, μ (ACI 11.6.3), was assumed to be 0.6 for the hairpin portion of topped hairpin & ductile ladder connectors, which simulating the ACI condition of concrete placed against hardened concrete not intentionally roughened. As for the ductile ladder portion of the topped hairpin with ductile mesh connector and for the ductile ladder connector alone tests with no tensile gap, a value of μ = 1.4 was used to simulate the ACI condition of concrete placed monolithically.

Table 6-6: Capacity Formulation Estimates

Connector	Ultimate Capacity, Pu
E: Topped Hairpin & Ductile Ladder (equation 1)	$f_u \cdot A_s \cdot \cos 45° \cdot \mu 1 + f_{wwr1-y} \cdot A_{s\_wwr1} \cdot \mu 2$ [μ1=0.6] [μ2=1.4]
E: Topped Hairpin & Ductile Ladder (equation 2)	$f_u \cdot A_s \cdot \cos 45° \cdot \mu + 0.8 \cdot f_{wwr1-u} \cdot A_{s\_wwr1} \cdot + A_c \cdot K_1$ [μ=0.6]

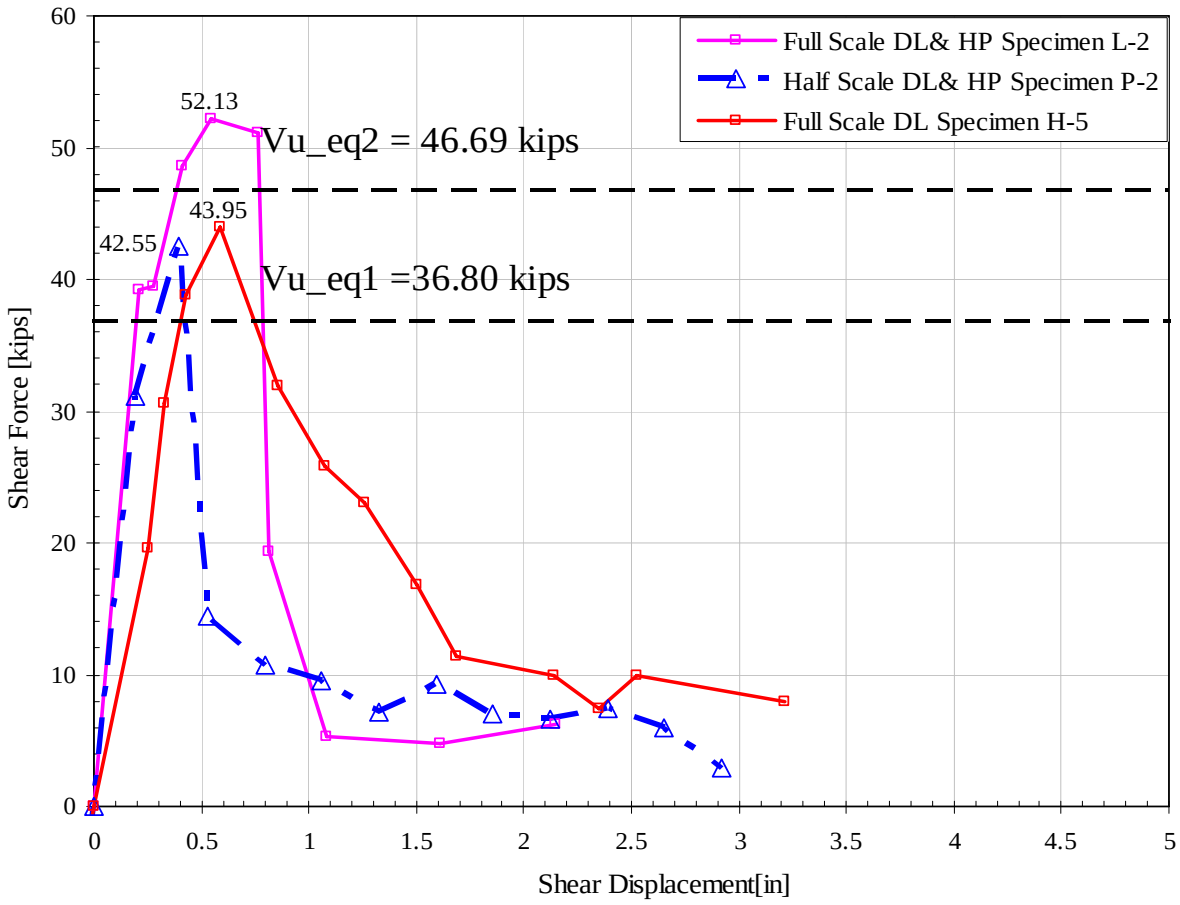

Figure 6-19: Cyclic Shear envelope comparison of specimen P-2 and specimens L-2 and H-5

As indicated in Figure 6-19, the measured capacity of the connector in shear was approximately 15% over the ultimate capacity when using equation 1, and was approximately 91% of the ultimate capacity calculated using equation 2 according to ACI design standards, in which the first term considered the contribution of friction to shear-transfer resistance and the second term represented the sum of the resistance to shearing of protrusions on the crack faces and dowel action of the reinforcement.

Compared with the bare ductile mesh test, the shear force capacity was decreased from 43.95 kips to 42.55 kips. Also, the shear deformation corresponding to the maximum force capacity and deformation capacity of half scale topped hairpin with ductile mesh connector test were also a little lower than bare ductile mesh connector, this may be caused by the a thicker 4-in pre-topped concrete panel contribution of bare ductile mesh connector. It is also can be referred that the hairpin connector can not contribute much to shear force and deformation capacity.

Compared with the half scale test, the shear force capacity was increased from 42.55 kips to 52.13 kips and the shear deformation corresponding to the maximum force capacity was increased from 0.4-in to 0.55-in., but both tests have a similar post-peak behavior followed by a steep drop of force capacity right after the peak load point.

The equation 1 (Dt =0 in) ACI shear friction model that was used to obtain the ultimate capacity does not accurately account for the concrete bearing contribution to the shear stiffness. The equation 2 ACI shear friction model has a separate component that more accurately calculates the shear resistance provided by the concrete, and does a better job in capturing the concrete contribution. This result in a conservative estimate of the shear capacity of the ductile

ladder utilizing equation 1, and a higher estimate of the shear capacity of the ductile ladder utilizing equation 2. The connector strength was between the tow calculated models.

As for the failure modes, both tests failed due to the fracture of ductile ladder strands and legs of hairpin connector.

6.4. Summary Comparison of Hairpin and Ductile Ladder Specimen at Full Scale and Half Scale

As discussed in this section, specimen P consisted of a half-scale hairpin and a full scale ductile ladder with less amount of steel crossed the joint. Consequently it was difficult to directly compare the results of this test series with previous full-scale test data. Instead the experimental results were compared with previous tests conducted on a hairpin connector and another test conducted on a ductile ladder connector. The data is also compared with previous analytical predictions based on ACI 318[1] for shear test since the data of previous tests with similar loading protocol are not available.

The comparison shows that for tension test, the force capacity and deformation capacity both match well with the previous tests. As for the shear test results, which are compared with previous analytical predictions based on ACI design equations, the connector attained the design strength value, and both the half scale and full scale tests have a similar post-peak behavior followed by a steep drop of force capacity right after the peak load point and a similar failure mode.

Since the half Scale topped hairpin with ductile mesh connector was composed of a half scale hairpin and a full scale ductile ladder connector with less amount of steel crossing the joint. It is hard to tell exactly the scale effect, but it still can be referred that for both cyclic tension and cyclic shear test of topped hairpin with ductile mesh connectors, the scaling did not affect much about the response behavior and failure modes of the connector, it is reasonable to use the results.

7. TYPE Q: HALF SCALE PRETOPPED D CARBON CHORD CONNECTOR

The pretopped carbon chord connector was developed in response to the poor performance of the pre-topped chord tested as part of phase 1A, which is summarized in ATLSS report 06-03[8]. The connection utilizes an unbonded region to enhance the tension ductility of the connection and to allow for shear compliance (i.e., shear movement with low force resistance). The chord is fabricated from ASTM A36 plate and ASTM A706 reinforcement. All welds were conducted at room temperature using E7018 or E90 electrodes via the SMAW process. The welds were sized to produce failure of the reinforcement prior to the welds. A 2-in thick pre-topped flange was chosen to represent half scale of a typical 4-in pre-topped diaphragm panel used in low seismic zones, and 2-in unbonded region was chosen to represent a half scale of 4-in unbonded length. As for the connector, the size of the reinforcing bar was scaled down from # 5 to #3; however, the number of the bars was increased from 2 to 6, so the reinforcing area is 106% of the previous the full scale specimen. The full scale and half scale connector details are shown in Figure 7-1 and Figure 7-3 respectively.

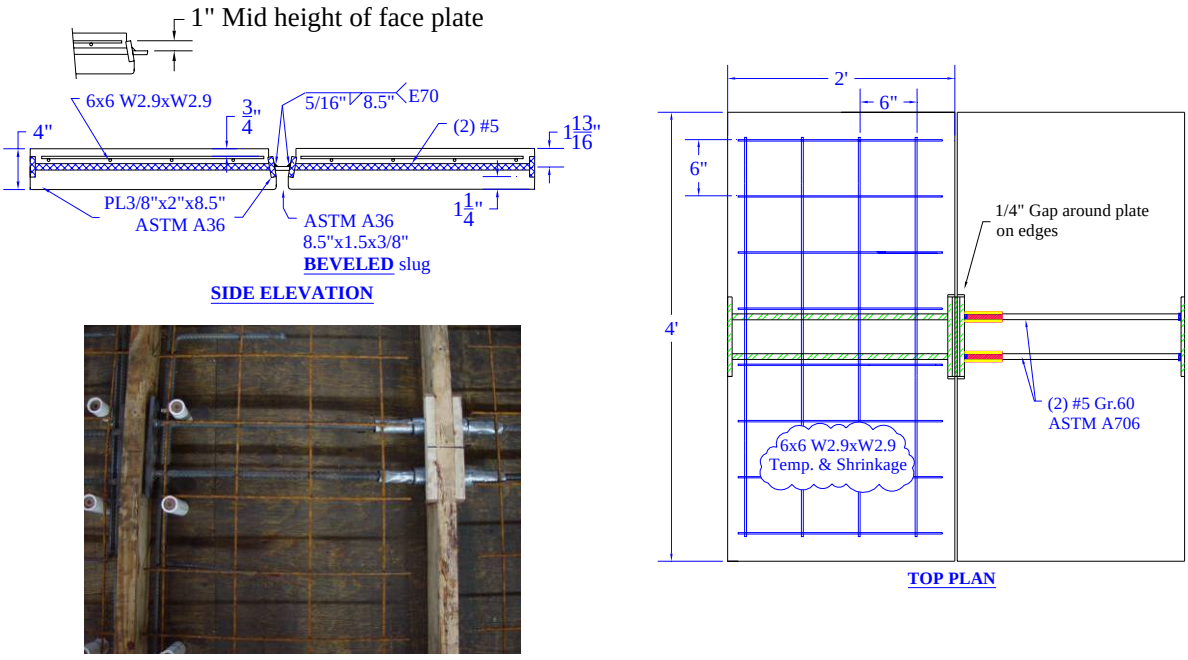

Figure 7-1: Full Scale Pre-topped Carbon Chord Connector (Type I)

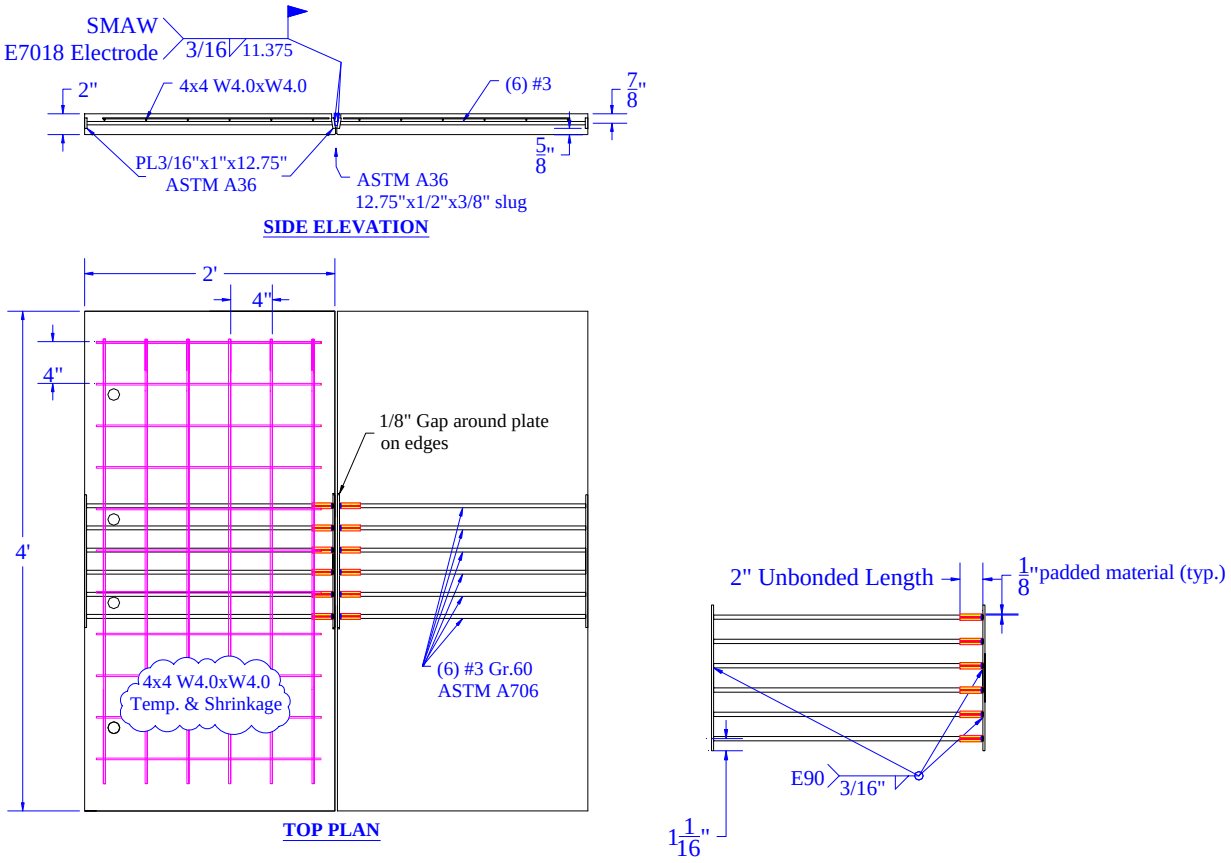

Figure 7-2: Half-scale Pre-topped Carbon Chord Connector (Type Q)

7.1. Material Properties of Half-Scale Pretopped Unbonded Carbon Chord

The 2-in. precast concrete panel was fabricated using high early strength self consolidating concrete with a design strength of 6000 psi. The WWR used in the base panel met the requirements of ASTM A185 grade 65 steel. The connector was fabricated from ASTM A706 grade 60 reinforcing bars. All plate and slug material conformed to ASTM A36. The compressive strength of the concrete when the panel tests were conducted was measured in accordance with ASTM C39. The measured concrete strengths and mill certified steel properties are presented in Table 7-1.

Table 7-1: Material Properties Capacity

Concrete Panel Type	28-day Compressive Strength, f'c [psi]			
2-in.	6003±53			
Size	Reinforcement Usage	Grade	Yield Stress [ksi]	Ultimate Strength [ksi]
#3	Connector	A706	65.6	94.3
PL 3/16" x 1" x 12.75"	Faceplate	A36	47.9	69.7
PL 1/2" x 3/8" x 12.75"	Slug	A36	47.9	69.7
#4	Reinforcing Bars	A615 Gr. 60	67.7	105.4
4X4 W4.0XW4.0	Pre-cast Panel Mesh	A185 Gr.65	65.00*	108.5
* Data unavailable, value assumed				

7.2. Type Q-1: Pretopped Carbon Chord Cyclic Tension with Fv = 0

The performance of the Carbon Chord connection subjected to cyclic tension and compression is presented in this section. The panel was subjected to axial displacement with the shear displacement unrestrained, Fv=0. For clarity the behavior is presented with respect to the panel location. The top is referred to as panel A and the bottom as

panel B. A reference tension deformation of 0.115 was used for the test, this value was based on the effective tension yield deformation of the half scale pretopped carbon chord connector, which was computed as half of the intercept of a horizontal line at the max load and a secant stiffness line at 75% of the max load of the full scale pretopped carbon chord connector under the monotonic tension loading protocol. Damage to the panels initiated with several hairline cracks forming in the concrete parallel to the joint and perpendicular to the joint in the tops of the panels. Next, yielding of the legs in tenson and buckling of the legs in compression resulted in spalling and delamination to occur on Panel A and then on Panel B as the test progressed. The connection ultimately failed with bar fracture of the carbon chords in Panel A at an opening displacement 0.69-in. Observed key events and the corresponding displacement level are presented in Table 7-2. The photos of the damage are presented in Figure 7-3 and Figure 7-4. The global force deformation response and backbone curve are presented in Table 7-3 and Figure 7-5.

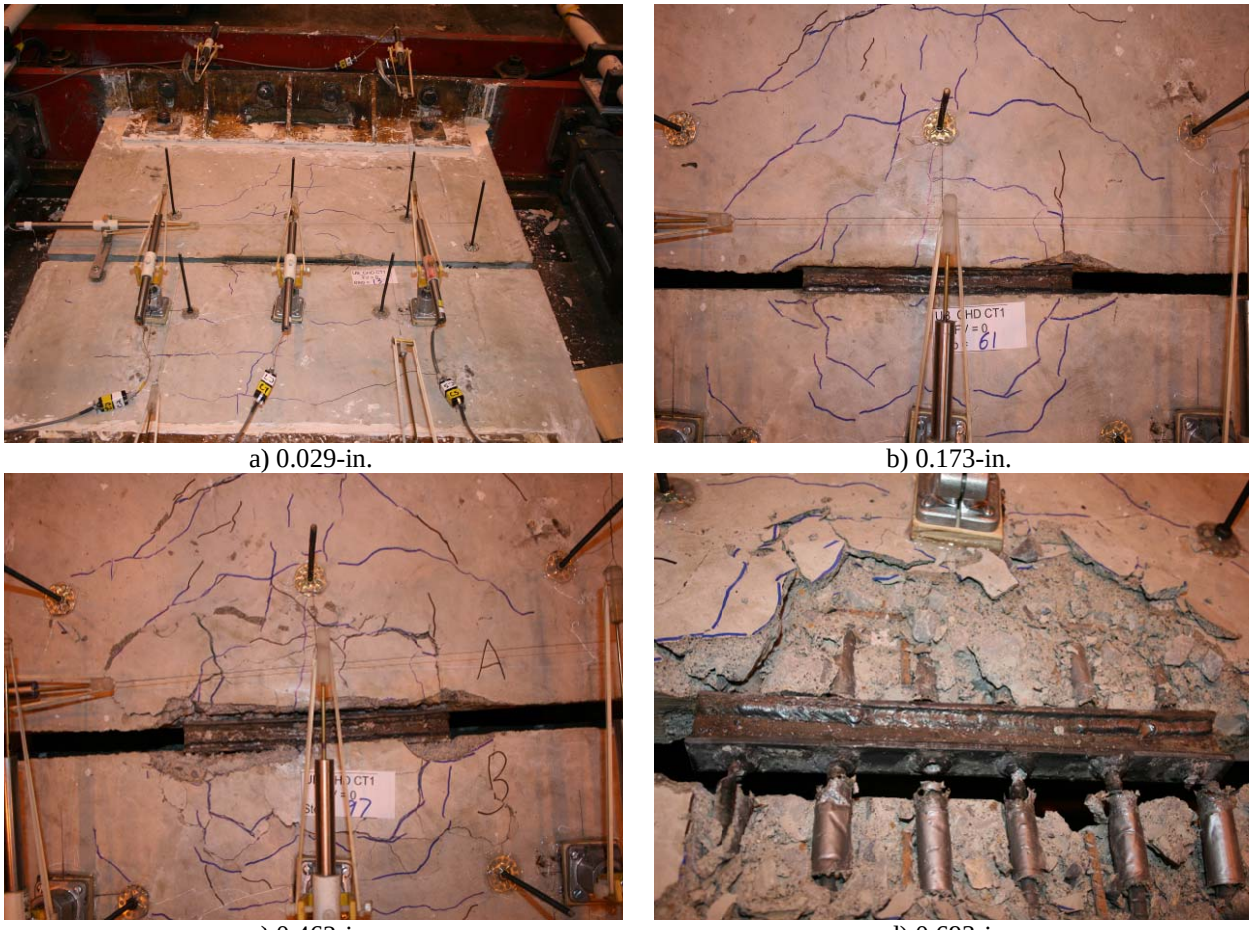

a) 0.029-in. b) 0.173-in.

c) 0.462-in. d) 0.693-in.

Figure 7-3: Damage state at various axial deformations.

a) 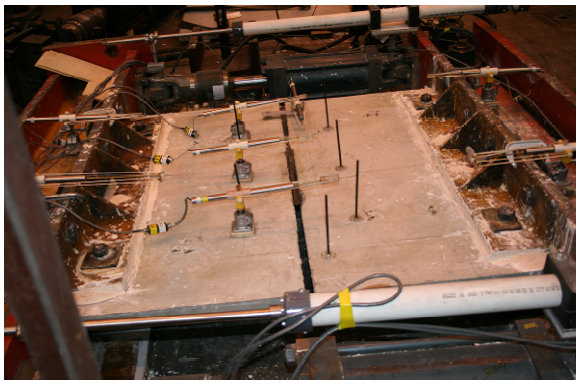 b) 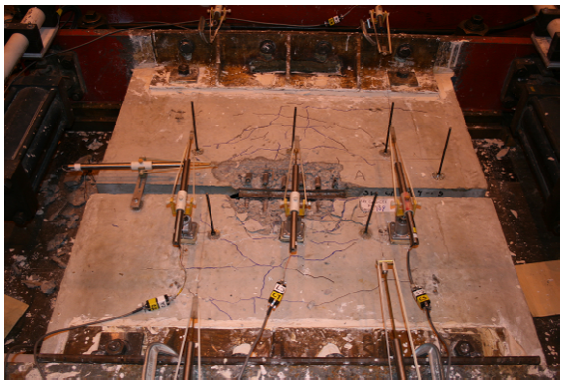

Figure 7-4: Initial and final overall condition.

Table 7-2: Key Test Observations (Cyclic Tension)		
Event #	Tensile Δ Step [in.]	Event Description
1	0.029	Cracks parallel and perpendicular to the joint formed on both panels
2	0.173	Loud noise heard, the concrete over the right leg of the connector on Panel A spalled
3	0.231	The concrete over the right side of the connector spalled on both panels, gaps occurred between the faceplate and panel
4	0.346	Existing cracks elongated, new additional cracks Increased separation between connector plates and concrete
5	0.462	Concrete around the joint lifted up, the third chord(from the right side) of connector A fractured(visible), all the rebar came out, the end is visible
6	-0.010	During compression steps, Concrete around the joint crushed
8	0.693	Failure in rebar on Connection A End of Test

Table 7-3: Experimental Results Backbone Curve (Cyclic Tension)		
Event	Tensile Displacement [in.]	Tensile Force [kips]
-	-0.003	-5.253
-	0.016	25.972
- Cracks formed on both panels	0.038	34.612
- The existing cracks elongated and additional cracks formed	0.058	40.723
	0.077	45.029
-Cracks elongated	0.120	49.596
-	0.190	48.533
-Peak Load	0.299	52.411
-	0.443	48.181
-Concrete around the joint lifted up, the third chord bar (from the right side) of connector A fractured(visible), all the rebar came out, the end is visible	0.453	26.085
-	0.578	20.717

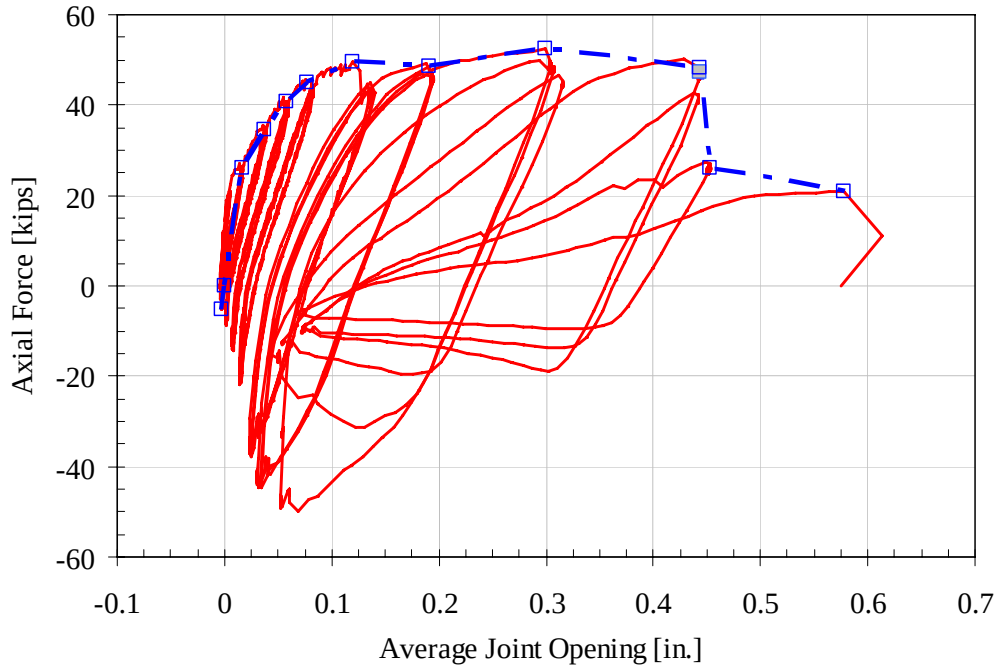

Figure 7-5: Axial Force and Axial Displacement for Pretopped Carbon Chord Connector

7.3. Comparison between Full Scale and Half Scale

The half scale specimen response compares well with previous full scale test results. As indicated in the section 7.1. the unbonded chord connector was composed of 6 pieces of # 3 rebar with a total area of reinforcement 0.66 $in.^2$ compared with the full scale unbonded chord connector test (2 # 5 bars) with a total area of reinforcement 0.62 in^2 test completed in Phase 1B. The ratio of the area of full scale connection to area of the half scale connection is 0.94, so the force scale factor for half scale to full scale is 0.94; while the length scale factor is 1 since the length of the chords was not changed. Then the results from the half scale tests were scaled to full scale by multiplying the displacements by 1 and forces by 0.94 in accordance with principals of similitude. Also, it is noted that the concrete panel of half scale test is 2-in, and the unbonded length 2-in was also half of full scale test, this also should be considered qualitative into the comparison. The connector performance is displayed in Figure 7-6.

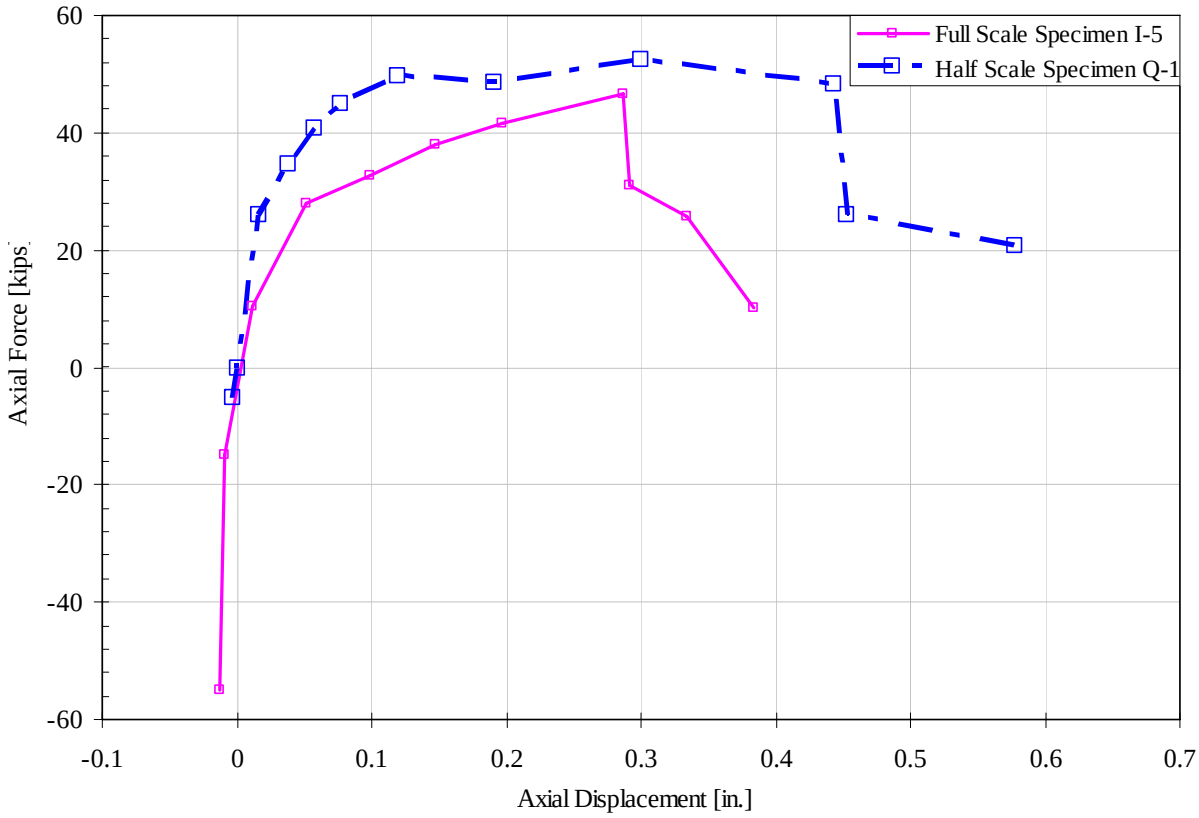

Figure 7-6: Cyclic Shear envelope comparison of specimen Q-1 and specimen I-5

Compared to the full scale test, the maximum force capacity in the scaled "half-scale specimen" was almost same at 49.6-kip, which was 78% of the ultimate capacity and 125% of the design capacity according to PCI design standards [11]. The PCI design and ultimate strength equations are summarized in summarized in ATLSS Report 07-04 [7]. The connector achieved the expected PCI design strength but did not match the ultimate strength. As for the shear deformation capacity, the deformation corresponding to maximum force capacity of both tests was also exactly same at 0.29-in, but the half scale test exhibited better deformation ductility, the shear deformation capacity was increased from 0.38-in to 0.54-in, and the ductility performance may be related to the failure modes (Figure 7-7). For the half scale test, the connector failed as desired bar failure, however, for the full scale test, the connector bars did not fracture from pure tension as desired, but failed due to bar-to-faceplate weld failure, despite design of the weld to resist bar fracture strength. The weld failure of full scale test was caused by poor quality control, which resulted in the fillet weld undersized at 67% of the design requirement, the connector performed well until the weld failed prematurely. So this may caused the higher ductility of half scale test.

a)Full Scale Test of Unbonded chord Connector

b) Half Scale Test of Unbonded chord Connector

Figure 7-7: Failure Modes of Half Scale and Full Scale Cyclic Tension Test of Pretopped chord Connection

7.4. Summary Comparison of Pretopped Carbon Chord Specimen at Full Scale and Half Scale

As indicated in this section, the ratio of the area of full scale connection to area of the half scale connection is 0.94 and the length of the chords was same as that of full scale connector, but the unbonded length and thickness of concrete panel were exactly half scaled, so it is hard to tell exactly the scale effect, but the scaled force capacity of half scale test compare well with the full scale test. So it can be referred that the scaling did not affect much about the response behavior and failure modes of the connector, it is reasonable to use the results.

8. Half-Scale Summary

This phase 1C test series examined the local performance of three diaphragm connection details at half scale. These include:

- JVI carbon steel vector connector
- Topped hairpin with ductile mesh
- Pretopped carbon chord connector.

The connectors were tested at half scale to replicate the details used in a shake table specimen examined at the University of California San Diego and the Phase 2 joint tests conducted at Lehigh University. It was found that in general all connectors displayed acceptable behavior under cyclic shear loading protocol with load capacities above design values and deformations in excess of 1/2-in. before complete strength loss. However, it is hard to get a general rule of connector performance under tension loading protocol since the modes of response and failure vary with each connector configuration. For example, the splayed leg connector such as JVI vector connector failed in low-cyclic fatigue modes, without achieving its design strength but displaying a good ductility up to 1.2 in. The topped hairpin with ductile mesh connector has the similar performance behavior as JVI connector. The straight leg connector such as unbonded chord connector exhibited tension capacities in accordance with their design values and the unbonded region improved the ductility performance. The details of connection behavior under shear and tension are illustrated in Figure 8-1and Figure 8-2.

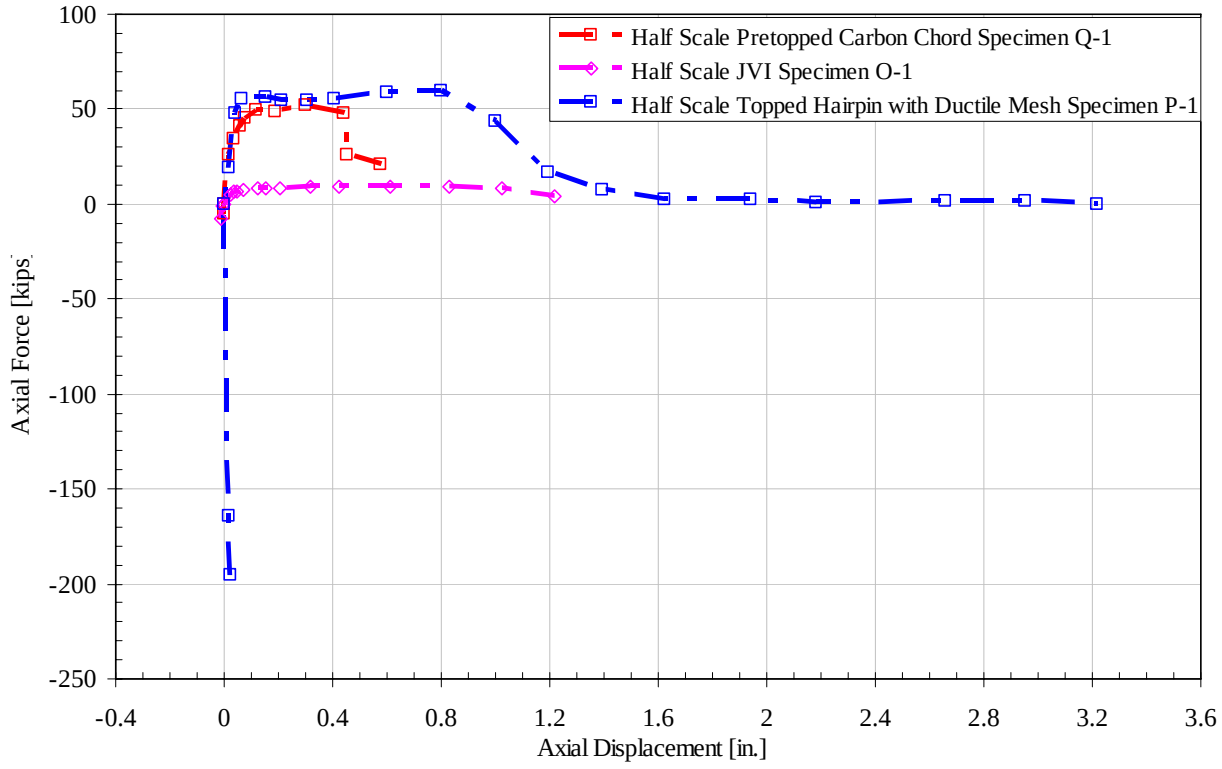

Figure 8-1: Cyclic Tension Envelops of Half Scale Connections

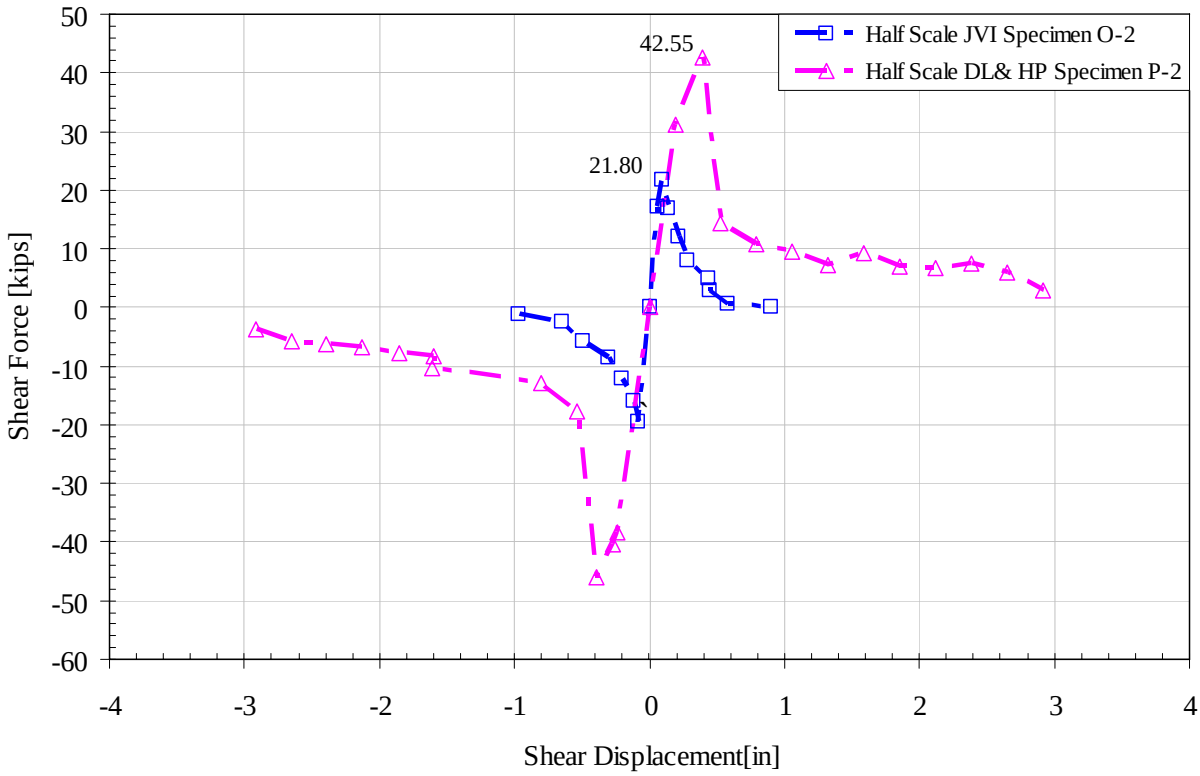

Figure 8-2: Cyclic Shear Envelops of Half Scale Connections

Based on the comparison between the results of half scale tests and full scale tests it is argued that the scaling did not significantly affect the behavior and failure modes of the connectors. Such as for JVI vector connector, which was tested at an exact half scale, the performance matched well with the full scale test, and both failed at a low cycle fatigue modes. For the topped hairpin with ductile mesh connector and unbonded chord connector, which were not exactly half scale, it can be concluded that the scaling effect was very small. The measured capacities are compared in Table 8-1.

Table 8-1: Results comparison of half scale tests and full scale tests

Connector	Test Condition	Load Capacity of Half scale Test [kip]	Equivalent Capacity of Full scale Test [kip]	Real Load Capacity of Full scale Test [kip]	Full Scale Design Value [kip]
JVI	CT	2.25	8.90	7.35	-
	CV	5.45	21.80	18.65	19.1*
Topped hairpin & ductile mesh	CT	14.87	-	-	25.9
	CV	42.55	-	-	36.8
Unbonded Chord	CT	52.41	49.27	49.62	-

* The deign value is from JVI Vector Inc[12]

9. REFERENCES

1. ACI 318, Building Code Requirements for Structural Concrete and Commentary, American Concrete Institute, 2005

2. Priestley, M.J.N., "The U.S. –PRESSS Program Progress Report," Third Meeting of the U.S. –Japan Joint Technical Coordinating Committee on Precast Seismic Structural Systems (JTCC-PRESSS), San Diego, CA, November 18-20, 1992.

3. American Society of Civil Engineers, Seismic Rehabilitation of Existing Buildings, ASCE Standard No., ASCE/SEI 41-06, 2007.

4. Federal Emergency Management Agency, "NEHRP Commentary on the guidelines for the seismic rehabilitation of buildings", Nov 2000

5. Naito, C., Ren, R., "Evaluation Methodology for Precast Concrete Diaphragm Connectors based on Structural Testing," The 14th World Conference on Earthquake Engineering, Beijing, China, October 12-19, 2008

6. AWS Structural Welding Committee, "AWS D1.4-92 Structural Welding Code," American Welding Society, Miami, FL, 1992.

7. Naito, C., Ren, R., Jones, C., Cullen, T., "PCI/NSF Development of a Design Methodology for Precast Concrete Diaphragms: Connector Performance Phase 1B," ATLSS Report 07-04, Lehigh University, Bethlehem, PA, June 2007

8. Naito, C., Peter, W., Cao, L., "PCI/NSF Development of a Design Methodology for Precast Concrete Diaphragms: Connector Performance Phase 1A," ATLSS Report 06-03, Lehigh University, Bethlehem, PA, Jan 2006

9. Amorn, A., Bowers, J., Girgis, A., and Tadros, M. K., "Fatigue of Deformed Welded-Wire Reinforcement", *PCI Journal*, V. 52, No. 1, Jan-Feb, 2007, pp. 106- 120

10. Plumtree, A., Abdel-Raouf, H.A., "Cyclic Stress-Strain Response and Substructure," *International Journal of Fatigue*, V. 23, 2001, pp. 799- 805

11. PCI Design Handbook, Precast and Pre-stressed Concrete, Fifth Edition, Chicago, IL, 1999

12. Oliva G.M., "Testing of the JVI Flange Connector for Precast Concrete Double Tee Systems," Laboratory Testing Report, University of Wisconsin-Madison, Jun 2000(available at www.jvi-inc.com)